

Climate Change in Norway and Effects on Terrestrial and Satellite Link Rain Attenuation

Kidist Yisfashewa Wondemu



Master Thesis
Signal Processing and Imaging
60 credits

Department of Physics
Faculty of Mathematics and Natural Science

Table of Contents

ABSTRACT	III
ACKNOWLEDGMENT	IV
1. INTRODUCTION.....	1
1.1. RADIO LINK DIMENSIONING.....	3
1.2. SPECIFIC RAIN ATTENUATION	3
1.3. TERRESTRIAL LINK RAIN ATTENUATION.....	5
1.4. SATELLITE LINK RAIN ATTENUATION.....	8
2. CLIMATE DATA ANALYSIS	11
2.1. THE IMPORTANCE OF CLIMATE PARAMETERS.....	11
2.2. METHODS OF CALCULATING RAIN RATE DISTRIBUTION	11
2.2.1. <i>Method based on tipping bucket data</i>	11
2.2.2. <i>Method based on monthly data</i>	14
2.3. METHOD OF DERIVING RAIN HEIGHT	15
3. RESULT OF CLIMATE PARAMETER ANALYSIS.....	17
3.1. REFERENCE TEMPERATURE AND DECADAL ANOMALIES	17
3.2. REFERENCE RAIN HEIGHT AND DECADAL ANOMALIES	18
3.3. SELECTION OF DIFFERENT LOCATIONS AND ESTIMATING CLIMATE DATA	20
3.4. SYSTEM PARAMETERS FOR THE TERRESTRIAL LINKS AND SATELLITE LINKS.....	23
3.5. RAIN HEIGHT AND RAIN RATE TIME SERIES	25
3.6. ATTENUATION TIME SERIES FOR TERRESTRIAL LINKS AND SATELLITE LINKS.....	28
4. DISCUSSION OF RAIN ANALYSIS AND FUTURE WORK	37
4.1. RAIN ATTENUATION IN TERRESTRIAL LINKS.....	37
4.2. RAIN ATTENUATION SATELLITE LINKS	38
4.3. ATTENUATION TREND LINE OVERVIEW	40
4.4. SUGGESTED FUTURE WORK	41
5. CONCLUSION.....	42
6. REFERENCE.....	44
ANNEX	47

Abstract

Radio technology has played a crucial role all over the world since its invention more than a century ago in everyday living. Terrestrial links are used for point-to-point radio transmission and satellite links are used for signal transmission between the earth and space. The objective of this thesis is to analyze whether climate change has an effect on the parameters rain rate and rain height for radio link design, i.e, rain attenuation. To analyze rain height and also temperature we have used ERA5 (the fifth-generation atmospheric reanalysis of climate data) database from the European Centre for Medium-Range Forecast (ECMWF), which provides monthly averaged data on single levels from 1950 to 2020. Then rainfall rate is analyzed from rainfall measurement tipping bucket data and monthly data from Seklima (Norwegian Centre for Climate Service). Rain attenuation is calculated by estimating climate parameters for several locations in Norway; Oslo, Kristiansand, Stavanger, Bergen, Trondheim, Tromsø and Vardø using prediction methods from the ITU-R (International Telecommunication Union Radiocommunication Sector). The result showed, the temperature anomaly increased by at least 1°C in the decade 2010 to 2019 in Norway and there is a rain height increase of up to 300 m in the selected locations. The northern part of Norway has shown a lower increase in rain height. And due to that, we have seen an increase in the attenuation trend in certain locations in four decades from the year 1980 to 2020. However, not all selected locations show an increase in attenuation from both the monthly data and tipping bucket data. When rain rate is derived by monthly data there are rain attenuation trend results, for all selected locations, except Bergen. In the terrestrial 18 GHz, 15 km link, the increase in rain attenuation is approximately 5 dB in the southern portion of Norway and even negative in Trondheim, but 1.5 to 2 dB in the north. In the terrestrial 38 GHz, 4 km link, the increase in rain attenuation is around 4 dB in the southern part, 1.3 to 2 dB in the northern part, and statistically insignificant in Trondheim. If data from tipping buckets are used to determine the rain rate for the 20 GHz satellite connection system, the trend line is only reliable for Bergen. Based on monthly statistics, rain attenuation increases by about 1 to 2 dB at lower elevation angles and by 2.3 to 2.4 dB at higher elevation angles. If the rain rate is calculated from tipping bucket data for the 50 GHz satellite connection system, this system has confident trend lines for Oslo and Bergen. Based on monthly data, rain attenuation increases from 8 to 13.7 dB at lower elevation angles and from 14.8 to 15.55 dB at higher elevation angles.

Acknowledgment

I am thankful to the almighty God for all things that have come into my life.

I would also like to thank my supervisor and co-supervisor for their excellent supervision. Associate Professor Terje Tjelta, I appreciate your patience, consistency, and tremendous assistance. I appreciate the contribution to MATLAB codes. He has devoted so much time and effort to follow me up. In addition, I'd like to thank Professor Sverre Holm, my co-supervisor, for his wonderful feedback. This master thesis would not have been accomplished without your help.

I would like to acknowledge Jostein Mamen for providing the rainfall measurement tipping bucket data.

In addition, I would like to thank my husband Addis Alemayehu and children for their patience, endless love and support. Many thanks to my mother and siblings and friends for their encouragement.

1. Introduction

Radio communication uses electromagnetic waves to exchange information. It has been more than 100 years since radio technology was invented. The terrestrial link has then become applicable for communication purposes. Radio had better capacity and flexibility than early days cable systems. It became preferable for certain parts of telecommunication systems. Then after the sixties, satellite communications are developed with much better connectivity with respect to reaching everywhere on the earth. This makes it easier to connect any point on earth with improved efficiency (Freeman, 2006; Loubere, 2021; Sizun, 2005).

In the 1990s the transmission using analog signals shifted to a digital signal. Even though most of the radio links have been replaced recently by fiber optics, it remains an important part of the telecom system. Fiber optics have now been used for the best speed and long-distance connection but also fiber to end-user homes. Mobile communication, wireless broadband communication and broadcasting have been used widely (Freeman, 2006; Hunsperger, 1995; Loubere, 2021; Sizun, 2005).

Outdoor radio systems are sensitive to weather conditions. The signal level and quality are the main requirements to design the system. We need to go to higher frequencies to increase the capacities, and it becomes more important to consider the possible effects of weather conditions. Many links today operate in the microwave band (>1 GHz) and millimeter wave (30 GHz to 300 GHz) frequency band. At frequencies above 10 GHz, hydrometeor precipitation often becomes the limiting factor. Hence rain attenuation limits the possible path length for the desired connection, for the necessary signal-to-noise ratio or higher capacity (Freeman, 2006; Kim et al., 2014; Sizun, 2005).

A point-to-point link is recognized by two antennas that are focusing on each other usually with a visible line of sight. The terrestrial link and satellite link are examples of point-to-point links. Its path is designed to operate short and long distances (Freeman, 2006; Sizun, 2005).

A terrestrial link is implemented to transmit signals between two points on the ground. The technique is different according to its application and efficiency. A terrestrial link is more advantageous for connecting irregular geographical areas. And it is applicable in radio

communication, mobile broadband and TV. It has less cost compared to a satellite link. The antenna that is used to receive/ transmit signals is usually directive and also mostly line of sight. The possible path length is dependent on location, frequency, the polarization of operation and link parameters e.g., antenna height, antenna gain and local climate condition. The operational frequencies are typically between 6 to 38 GHz but are not limited to it (Freeman, 2006; Sizun, 2005).

A Satellite link is used for the transmission of signals between the earth and space. The coverage area is much better than the terrestrial system. (Sizun, 2005). The ground reflection does not affect radio wave propagation while using a satellite link, since the elevation angles are above a few degrees. The most common application of satellites is communication technology, weather forecasting and earth observation. A communication satellite is mostly used for broadcasting. Recently in mobile communication, there is an increasing interest in using links with short-range both millimeter and submillimeter and terahertz. Satellites that are used for weather forecasting, scan the atmospheric parameter above the cloud for prediction. Whereas satellites for earth observation, navigate data from the earth by taking photographs of the desired region. The radio wave signal in satellite links above the frequency of 10 GHz, is heavily attenuated when we have rain or wet snow (Freeman, 2006; Maral & Bousquet, 2009; Sizun, 2005).

One of the main focuses of this thesis is to have a general view of radio wave propagation and the requirement for dimensioning to transmit signals from one point to another. It studies the climate change effects on the transmission of outdoor systems in Norway. The study is based on long-term climate data in Norway and identifies the effect on the radio system. This thesis analyses the effect of possible climate change on radio links, specifically rain attenuation. Two types of radio links are studied, one is terrestrial, and the other one is earth-to-space link or satellite connection. These two types have somewhat different methods on how to estimate rain attenuation. But for both, rainfall intensity must be analyzed well since it is an important factor for radio link dimensioning.

This study analyses the rainfall distribution and attenuation based on the method in ITU-R recommendation using the climate data from Norwegian meteorological institute, Seklima (Norwegian centre for climate service) (MET, 2022) and the European centre for the medium-range forecast (ECMWF), particularly from ERA5 (the fifth generation atmospheric

reanalysis of climate data) which gives monthly averaged data on single levels from 1950 to 2020 years (Bell et al., 2020; Hersbach et al., 2019; ITU-R, 2017a, 2017b).

1.1. Radio link dimensioning

In order to design a radio link, it is important to consider the range, capacity and performance of the link by checking the effect of radio wave propagation. Performance degradation can also be caused by an outage due to a weather change. One of the limitations is rain so in this study, we will only be concerned about that (Sizun, 2005).

There are different physical mechanisms of radio wave propagation. i.e., free-space propagation, line-of-sight propagation, reflection, diffraction, transmission, scattering and waveguiding (Freeman, 2006; Sizun, 2005). This effect must be considered for both terrestrial and satellite links since rainfall intensity and raindrops affects the signal. Rainfall and raindrop size varies with geographical locations.

The link quality is evaluated by availability and performance. It is done by evaluating the link that is available in time and checking the bit error ratio (BER). The link must have BER that is smaller than the threshold to avoid an outage. This leads to performance deterioration that results in the total cut-off transmission. Therefore, it is necessary to check the quality (Freeman, 2006; Sizun, 2005; Sklar, 2021).

A satellite link is sensitive to rain and due to that the signal is attenuated and the noise resulting from rain increases by a small amount (Freeman, 2006; Maral & Bousquet, 2009; Sizun, 2005). This affects the quality of the link. The vital prediction method to calculate satellite link performance that is a signal-to-noise ratio that is related to rain attenuation. The total signal-to-noise ratio is calculated by considering the uplink (from the ground terminal to the satellite) and downlink (from the satellite to the receiver) performance due to rain attenuation.

1.2. Specific rain attenuation

The propagation of radio waves is affected by rain for frequencies above 10 GHz (Freeman, 2006; Tjelta & Mamen, 2014). However, the ITU-R model that is used for the prediction of

rain attenuation is applicable for the frequency range of 1 GHz to 1000 GHz (ITU-R, 2005). Rain rate is the main climate parameter that increases the attenuation and depolarization of signals that reduce the link availability.

The method to calculate the specific rain attenuation γ uses rain rate and coefficients a and b from the table ITU-R recommendation P.838-3 and set it to the formula (ITU-R, 2005)

$$\gamma = aR^b \quad (\text{dB/km}) \quad 1.1$$

where R is rain rate exceeded in mm/h for 0.01% of an average year, a and b are dependent on polarization, frequency (GHz) and tilt angle. For example, (Olsen et al., 1978) showed that the power law can be used for the calculation. The coefficients a and b are frequency dependent. Some of these values were empirically determined and may contain inaccuracies, but have been revised several times and now use as in ITU-R P.838-3 (ITU-R, 2005). The equation gives a general relation, except for the low-frequency and optical limitations. The a and b values are given in tabular and graphical form for frequencies 1 to 1000 GHz. Figure 1.1 shows specific attenuation for different rain rates. We can see that specific attenuation increases with frequencies below 100 GHz and rain rate. And also, horizontal polarization has higher specific attenuation than vertical polarization.

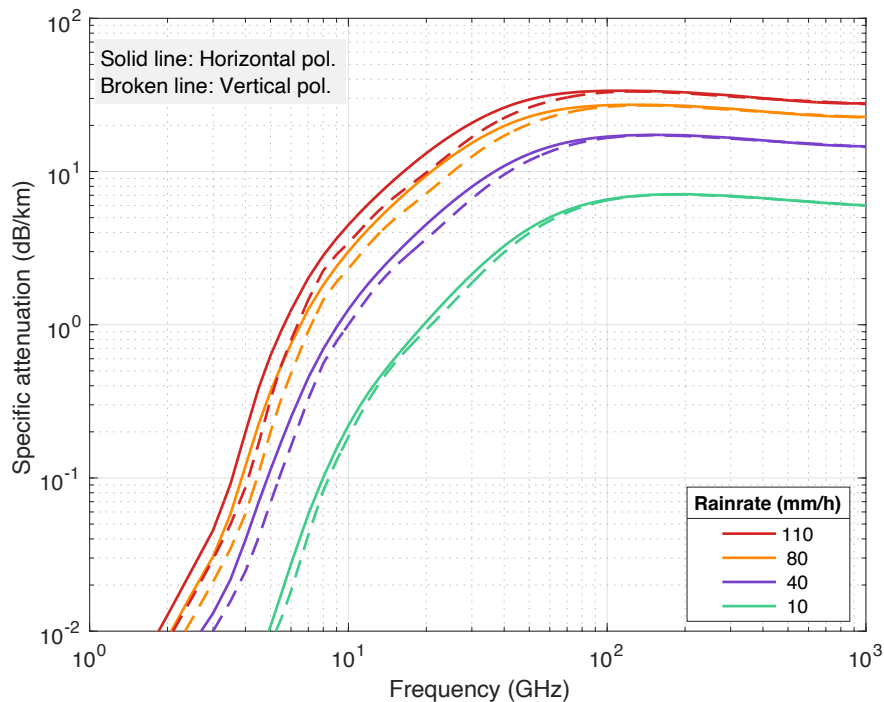


Figure 1.1 Example of rainfall rate and specific attenuation increases with frequency

1.3. Terrestrial link rain attenuation

The terrestrial path may be affected by climate change for frequencies higher than 10 GHz. This is due to the electromagnetic waves that interact with the atmosphere. That is mainly rain, snow, or hail. They have various effects on wave attenuation in the link performance (Freeman, 2006; Sizun, 2005).

The steps to predict rain attenuation in the terrestrial link by using the recommendation in ITU-R, P.530 are specified below (ITU-R, 2021).

- Step 1: Calculate the specific rain attenuation by using Equation 1.1
- Step 2: Calculate the effective path length by using path reduction factor r and the actual path length d of a terrestrial path.

$$r = \frac{1}{0.477d^{0.633}R_{0.01}^{0.073b}f^{0.123} - 10.579(1 - \exp(-0.024d))} \quad 1.2$$

$$d_{eff} = rd \quad 1.3$$

- where f (GHz) and $R_{0.01}$ is rain rate exceeded in mm/h for 0.01%.
- Step 3: Using effective path length and specific rain attenuation we can use this model to predict attenuation in dB related to percentage p (A_p) where p is between 0.001% and 1%.

$$A_{0.01} = \gamma d_{eff} \text{ (dB)} \quad 1.4$$

$$A_p = A_{0.01} c_1 p^{-(c_2 + c_3 \log p)} \quad 1.5$$

where $c_1 = 0.07^{c_0} (0.12)^{(1-c_0)}$, $c_2 = 0.855c_0 + 0.546(1-c_0)$, $c_3 = 0.139c_0 + 0.043(1-c_0)$ and $c_0 = 0.12 + 0.4(\log(f/10))^{0.8}$ for $f \geq 10$ GHz or 0.2 for $f < 10$ GHz

The climate parameter we need to consider for dimensioning terrestrial links due to rain attenuation is rain rate. Its effect on a terrestrial path is shown in Figure 1.2.

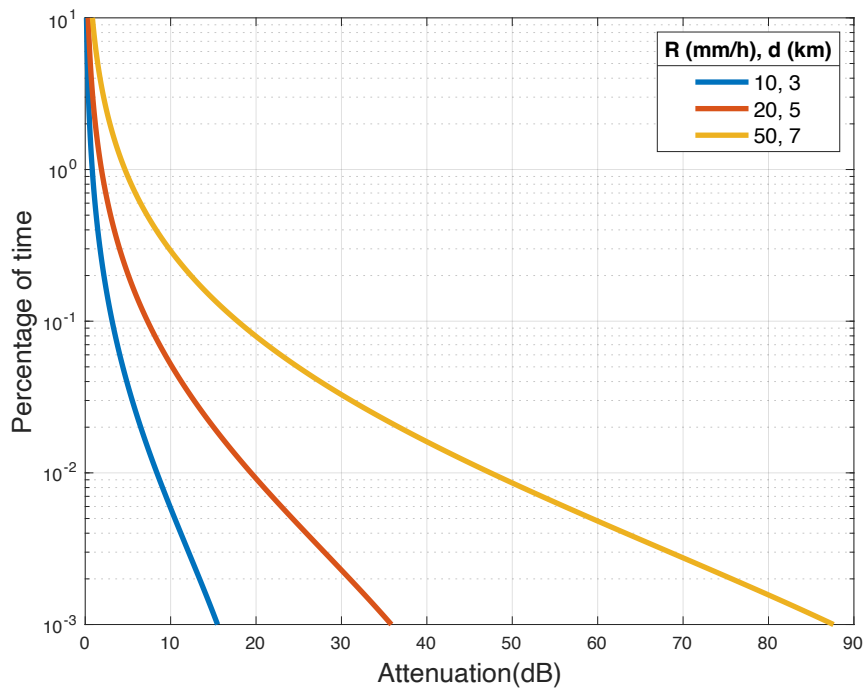


Figure 1.2. Example of attenuation and percentage of time for different rain rate (mm/h) 10, 20, 50 for distances 3, 5, and 7 km respectively

An example of complementary cumulative rain distribution in the percentage of time is shown in Figure 1.2 and Figure 1.3 for 38 GHz links of different path lengths compared with fixed rain rate (50 mm/h) and different path lengths.

In Figure 1.2, the link with a rain rate of 10 mm/h and a path length of 3 km has the lowest attenuation which is 16 dB with 99.999 % (0.001%) of availability. The link with a rain rate of 20 mm/h and a path length (d) of 5 km has rain attenuation of 36 dB, and for R= 50 mm/h, d = 7 km is 88 dB with 99.999 % (0.001%) availability.

In Figure 1.3 the three links have the same rain rate but different path lengths (3, 5, and 7 km) respectively. The longest path length is highly attenuated by rain.

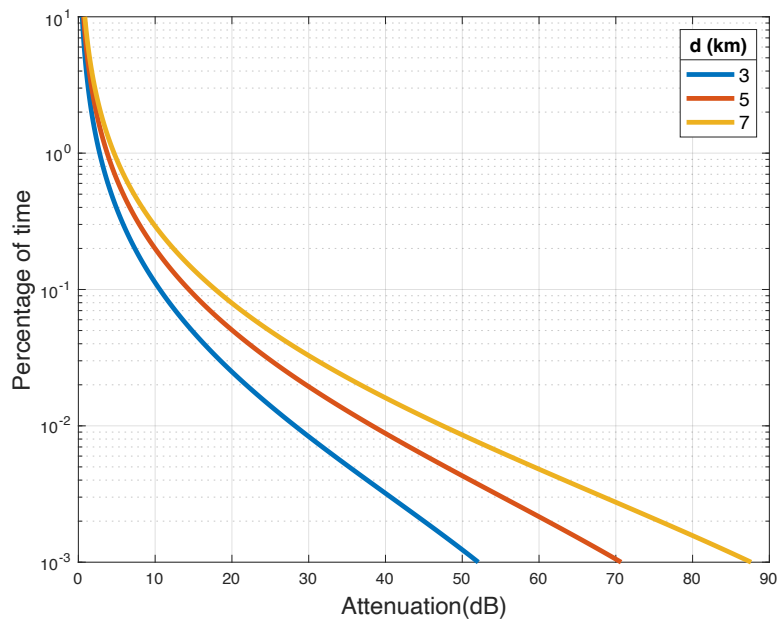


Figure 1.3 Example of attenuation for a 38 GHz link with a path length 3, 5 and 7 km at rain rate 50 mm/h

To clarify the effect of variability shown clearly for the 38 GHz link in Figure 1.4, rain attenuation increases when we increase path length and rain rate.

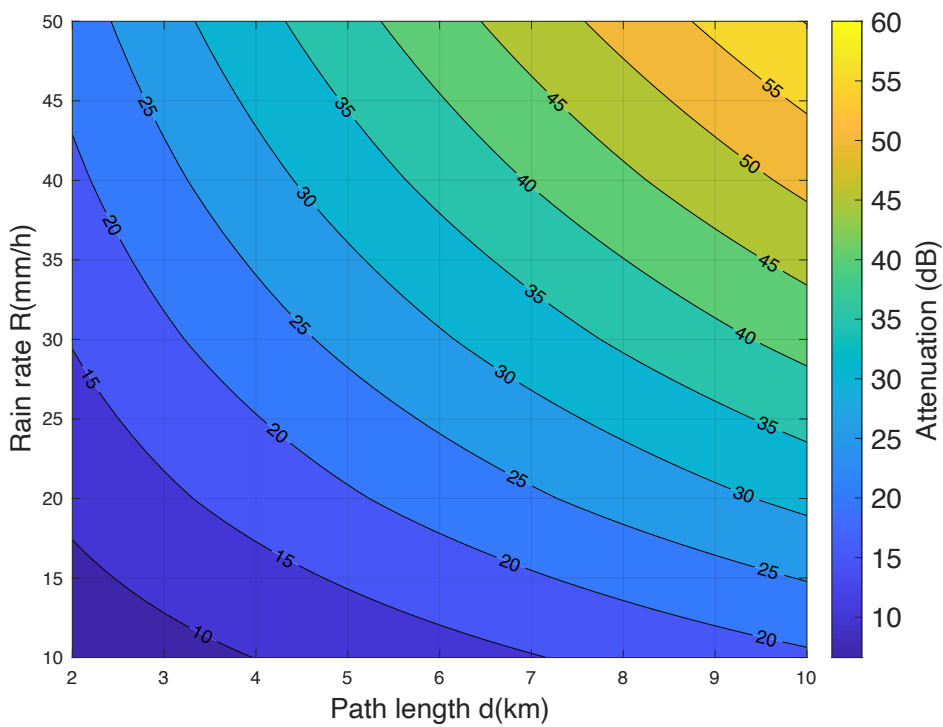


Figure 1.4 Example of rain attenuation for different rain rates and path length for a horizontal polarization 38 GHz link

1.4. Satellite link rain attenuation

By using a prediction method for satellite link rain attenuation that is recommended in ITU-R P.618-13, we will determine specific attenuation and the rain height (ITU-R, 2017b). The steps that are used to predict rain attenuation are illustrated below.

- Step 1: The rain height model that is recommended in ITU-R P.839-4 is used to calculate rain height (h_R) by considering h_0 (zero-degree height in m) isotherm for satellite links (ITU-R, 2013). The calculation is as follows.

$$h_R = \frac{h_0 + 360}{1000} \quad (\text{km}) \quad 1.6$$

- Step 2: The length through the rain (L_S in km) shown in Figure 1.5, is calculated in ITU-R P.618-13 by considering the elevation angle θ ,

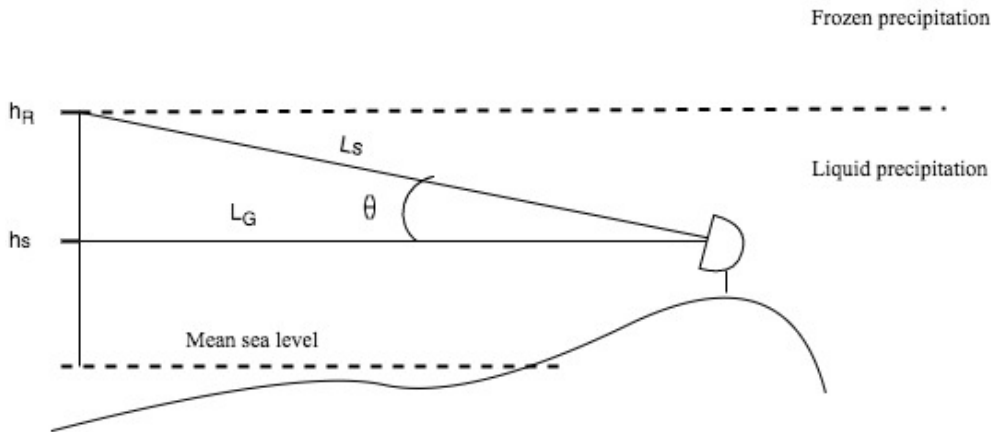


Figure 1.5 Geometry of earth-space path

the altitude of the melting layer (rain height h_R) (km) and height of the antenna h_S and R_e is the effective radius of the earth under a normal atmosphere (8500 km)

$$L_S = \begin{cases} \frac{h_R - h_S}{\sin\theta} & \text{for } \theta \geq 5^\circ \\ \frac{2(h_R - h_S)}{\sqrt{\sin^2\theta + \frac{2(h_R - h_S)}{R_e} + \sin\theta}} & \text{for } \theta < 5^\circ \end{cases} \quad (\text{km}) \quad 1.7$$

the horizontal length L_G (km) is $L_S \cos\theta$.

- Step 3: Calculate the specific attenuation (γ_R) in dB/km using Equation 1.1 from rainfall rate (R) dataset that is exceeded for 0.01% of an average year
- Step 4: The horizontal reduction factor ($r_{0.01}$) and vertical adjustment factor ($v_{0.01}$) are calculated by

$$r_{0.01} = \frac{1}{1 + 0.78 \sqrt{\frac{L_G \gamma_R}{f}} - 0.38(1 - e^{-2L_G})} \quad 1.8$$

$$v_{0.01} = \frac{1}{1 + \sqrt{\sin\theta} \left(31(1 - e^{-\left(\frac{\theta}{(1+x)}\right)}) \frac{\sqrt{L_R \gamma_R}}{f^2} - 0.45 \right)} \quad 1.9$$

where the angle ζ , L_R (km) and x are calculated by

$$\zeta = \tan^{-1} \left(\frac{h_R - h_S}{L_G r_{0.01}} \right) \quad 1.10$$

$$L_R = \begin{cases} \frac{L_G r_{0.01}}{\cos\theta} & \text{for } \zeta > \theta \\ \frac{h_R - h_S}{\sin\theta} & \zeta \leq \theta \end{cases} \quad 1.11$$

$$x = \begin{cases} 36 - |\phi| & \text{for } \phi < 36^\circ \\ 0 & \text{for } \phi \geq 36^\circ \end{cases} \quad 1.12$$

where ϕ is the latitude of the earth.

- Step 5: Then effective path length L_E is calculated

$$L_E = L_R v_{0.01} \quad (\text{km}) \quad 1.13$$

- Step 6: Attenuation for the percentage of the year (A_p) is

$$A_p = A_{0.01} c_1 \left(\frac{p}{0.01} \right)^{-(0.665 + 0.033 \ln(p) - 0.045 \ln(A_{0.01}) - \beta(1-p)\sin\theta)} \quad (\text{dB}) \quad 1.14$$

where $A_{0.01} = \gamma_R L_E$ and

$$\beta = \begin{cases} 0 & \text{for } p \geq 1\% \text{ or } |\phi| \geq 36^\circ \\ -0.005(|\phi| - 36) & \text{for } p < 1\% \text{ or } |\phi| < 36^\circ \text{ and } \theta \geq 25^\circ \\ -0.005(|\phi| - 36) + 1.8 - 4.25\sin\theta, & \text{otherwise} \end{cases} \quad 1.15$$

Figure 1.6 shows an example of the prediction of rain attenuation for Nittedal and Røst with parameters used in Table 1. Nittedal has a higher attenuation of about 29 dB for a percentage of 0.001% exceedance (99.999 %) whereas Røst has 18 dB for 0.001% exceedance.

	Nittedal	Røst
h_s (km)	0.2	0.01
θ (°)	21.8	14.1
$R_{0.01}$ (mm/h)	25.6	21.9
h_R (km)	2.29	0.88
f (GHz)	19.7	19.7

Table 1 Selected parameter for rain attenuation prediction

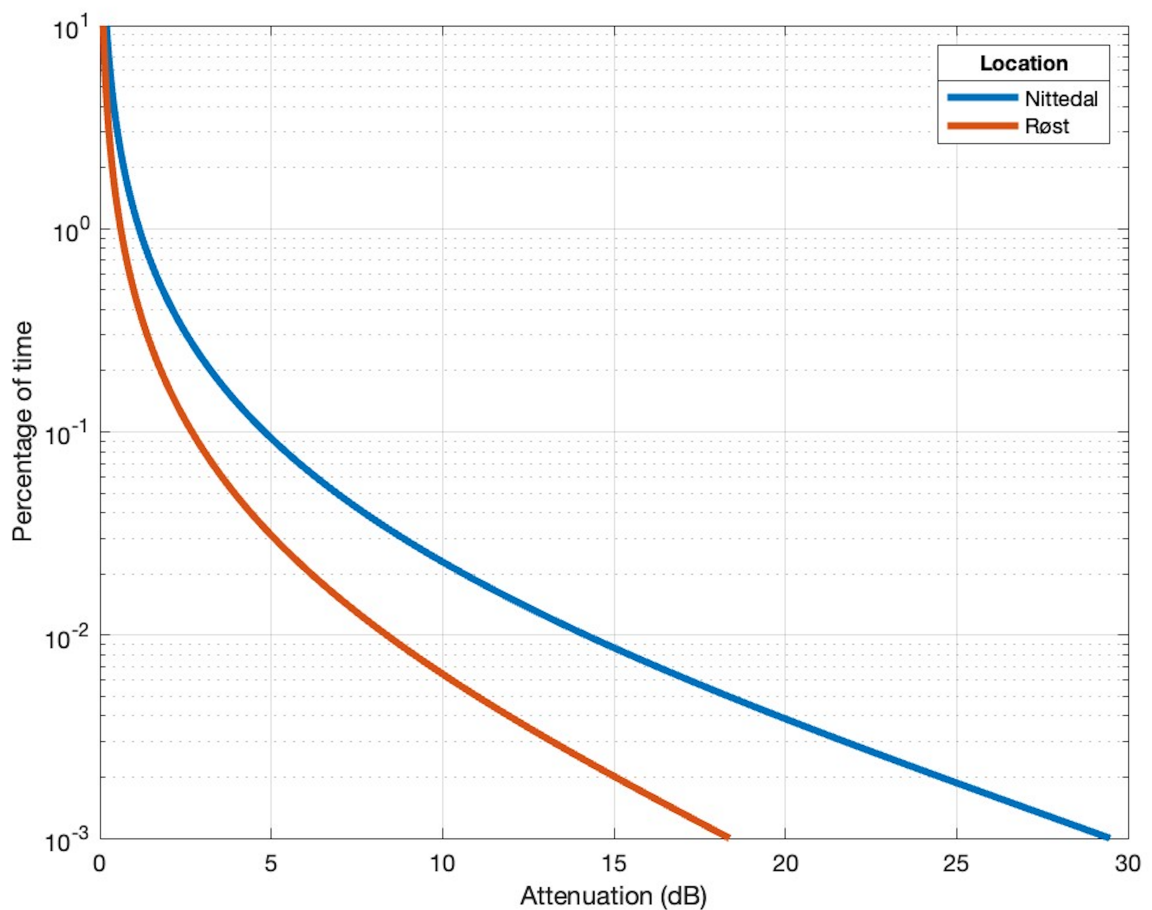


Figure 1.6 Example of rain attenuation for the sites Nittedal and Røst for a 19.7GHz horizontal polarization

Using the above prediction methods for both terrestrial and satellite links, rain attenuation is calculated for dimensioning radio links.

2. Climate data analysis

2.1. The importance of climate parameters

The two most important climate parameters for rain attenuation are rain height and rain rate. Rain rate is important for designing both terrestrial links and satellite links. whereas rain height is for satellite links.

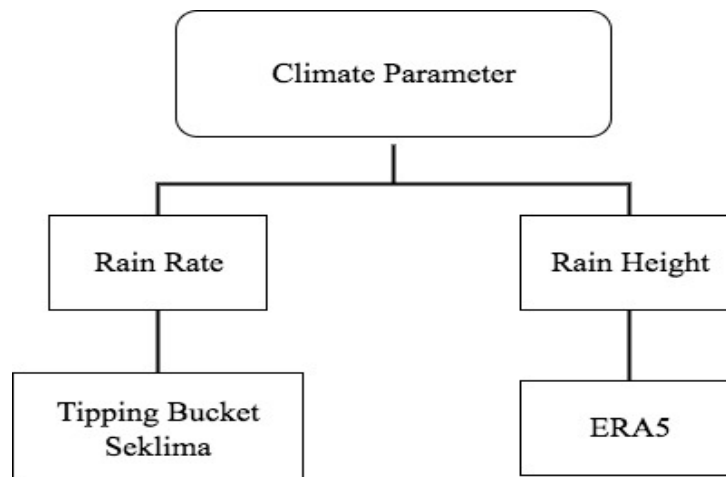


Figure 2.1 Flow chart of climate parameter

The flow chart shown in Figure 2.1 visualizes what is needed to predict rain attenuation for this study. We focus on the important climate parameter which is rain height and rain rate. Rain rate is calculated from the data from the tipping bucket and monthly data in (Seklima) whereas rain height is from ERA5.

2.2. Methods of calculating rain rate distribution

The rain data are analyzed from two sources. The first one is from tipping bucket data that is provided by the Norwegian Meteorological Institute (MET) starting from the year 1967 to 2020, and it is used to calculate the rain rate for each year. And the other one is also from the Met Office used in ITUR methods from monthly mean air temperature ($^{\circ}\text{C}$) and monthly precipitation (mm) (Bell et al., 2020; Hersbach et al., 2019; Mamen & Tjelta, 2013; Tjelta & Mamen, 2014).

2.2.1. Method based on tipping bucket data

MET measures rainfall intensity using tipping bucket equipment that counts the number of tips per clock minute (Mamen & Tjelta, 2013; Tjelta & Mamen, 2014). This means for each

minute the number of tips is registered and converted to mm/h. The bucket size that was used to collect rainfall was 0.2 mm and then changed to 0.1 mm.

The rainfall distribution algorithm to estimate rainfall distribution is in (Mamen & Tjelta, 2013). The study determines the distribution of rainfall rates during the period by using data from the rain gauges' tipping buckets. After interpolating the cumulative distribution of rainfall rates, the algorithm converts it to a number of tips to correct too low resolution in the data set and combine 0.2 mm and 0.1 mm buckets. The result of the analysis of rainfall that exceeded 0.01%, is used to calculate rain attenuation.

In Figure 2.2 we can see the measured rainfall (marked in blue) for each year. The green and red dots represent the starting and ending periods of the measurement (Tjelta & Mamen, 2014). In previous years, the measurement is done only during the warm period of the year. Whereas recently the instrument is modified to perform a measurement for the whole year (Mamen & Tjelta, 2013; Tjelta & Mamen, 2014).

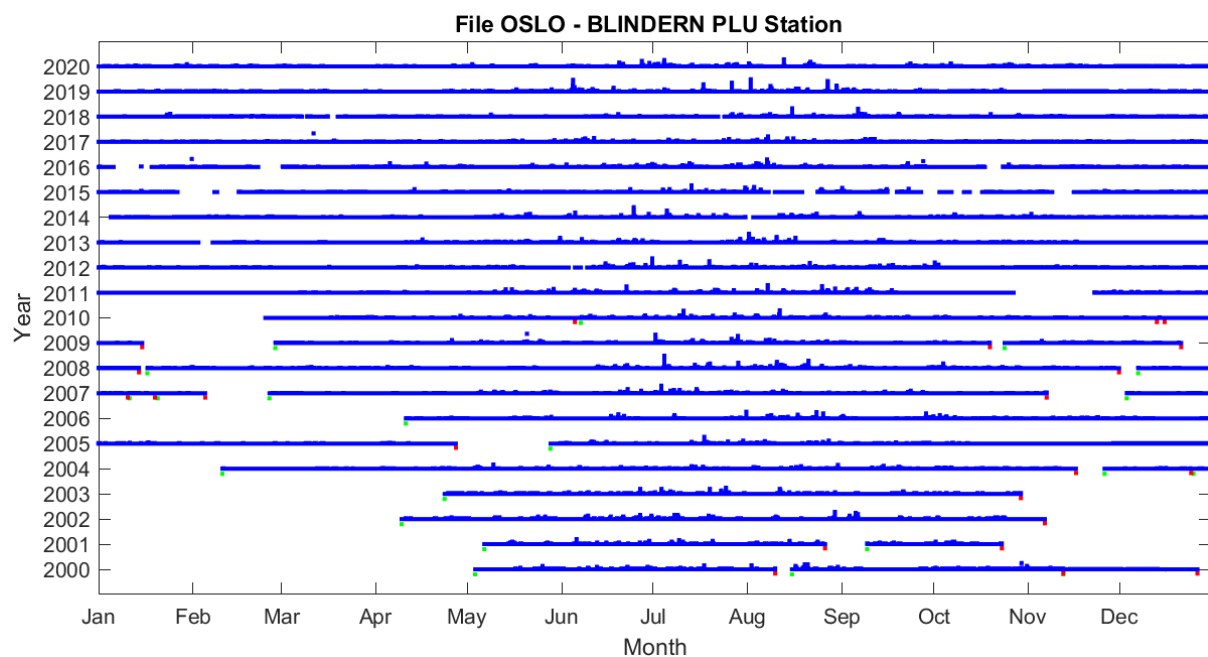


Figure 2.2 Rainfall data from tipping bucket in Oslo

Hence there are missing data in several sites and years due to wintertime or other reasons, but the highest intensity of rainfall is in the warm period. Rainfall in Hamar is recorded for the whole year after 2010 as shown in Figure 2.3.

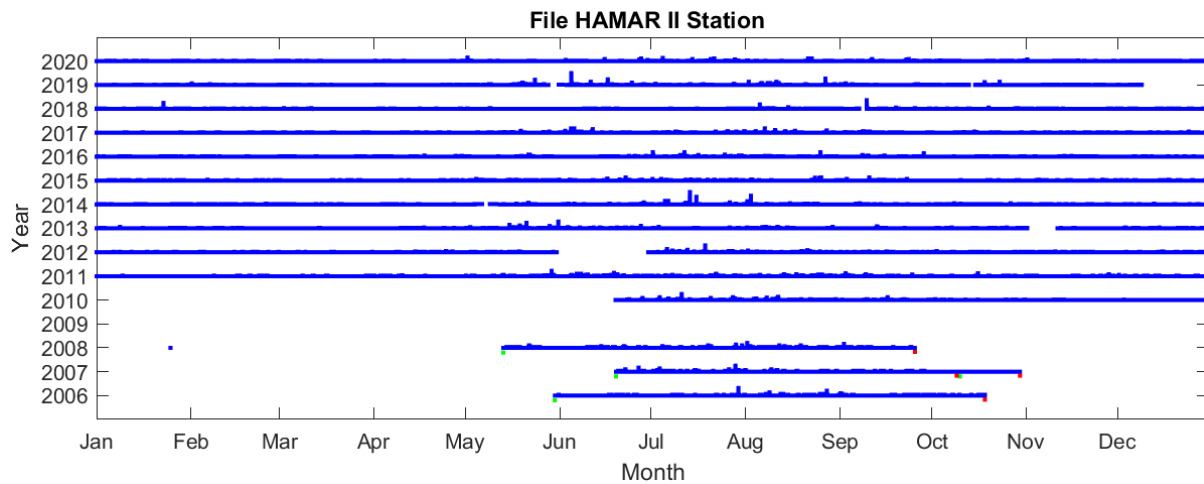


Figure 2.3 Rainfall data for Hamar II with a tipping bucket

The rainfall distribution is calculated from the data to show the percentage of time that is related to the rain rate for each location. From Figure 2.4 we can see the rainfall distribution in Oslo Blindern for the period 1968 to 2020. The rain rate that exceeded 0.1% is 10.9 mm/h and 0.01% is 30.6 mm/h and 0.001% is 69.2 mm/h.

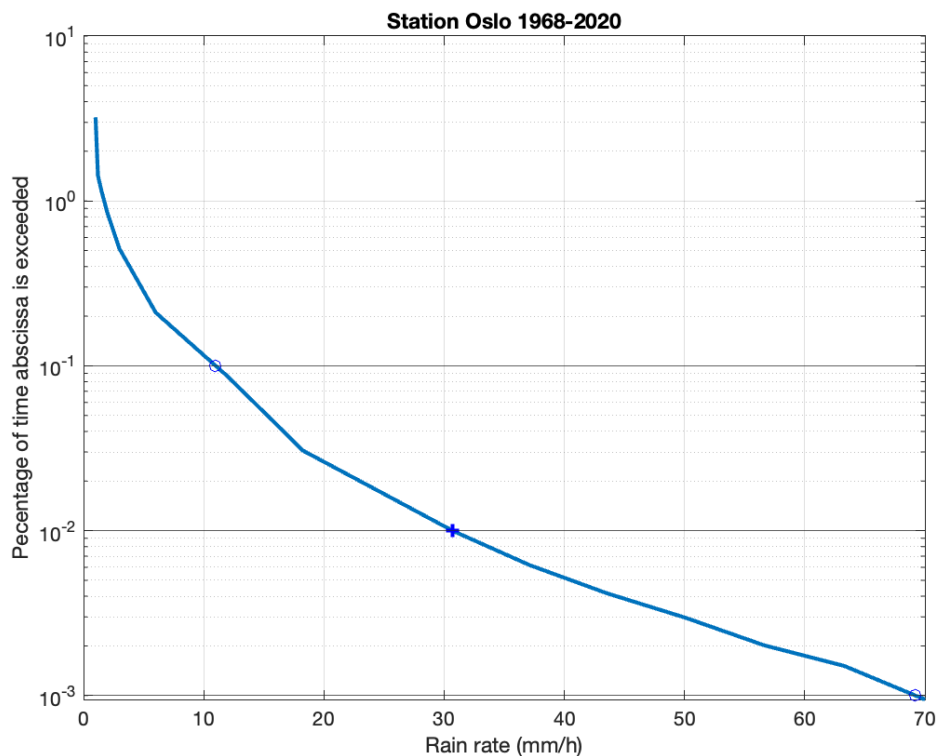


Figure 2.4 Rain rate distribution for Oslo Blindern with a tipping bucket data

The rainfall distribution for Hamar II is shown in Figure 2.5. The rain rate that is used for attenuation prediction methods is the rate exceeding 0.01% of the time to calculate specific attenuation shown in Equation 1.1, which is $R_{0.01} = 22$ mm/h for Hamar II.

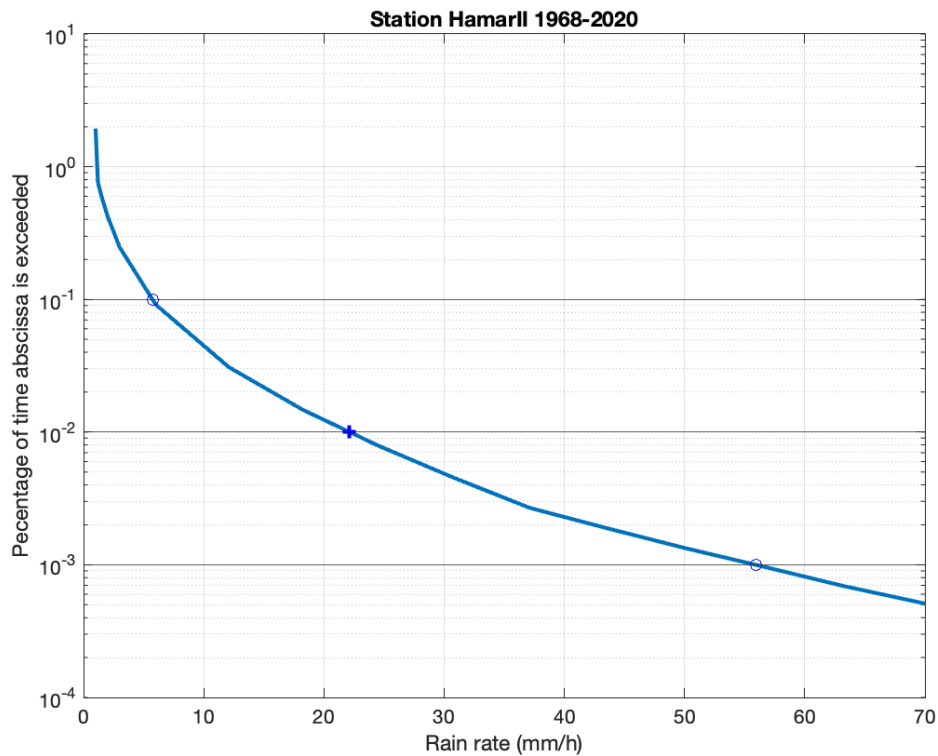


Figure 2.5 Rain rate distribution for Hamar II

2.2.2. Method based on monthly data

Monthly data are used to drive rain rate distribution by using a recommendation in ITU-R P.837-7 (ITU-R, 2017a, 2020). The background material and validity checking are found in (ITU-R, 2020; Jeannin et al., 2013). The data from the Norwegian centre climate service (Seklima) (MET, 2022), i.e, monthly mean air temperature (°C) and monthly precipitation (mm) are downloaded for rain rate calculation.

The recommendation model P.837-7 is used for the rain rate distribution from monthly data as well as the tipping bucket data (ITU-R, 2017a, 2020). The recommendation proposes the prediction of rainfall rate statistics when reliable long-term local rainfall rate data are lacking. This prediction method is based on total monthly precipitation data and monthly mean surface temperature data. The calculated rainfall rate using this model with monthly data from Seklima and tipping bucket data are compared as shown in Figure 2.6. The rain rate distributions are comparable however for Oslo the rates found from tipping bucket data are somewhat larger than monthly data at the same percentage of the time. The rain rate at 0.01%

of the time (marked with a cross in the figure) is used to calculate specific rain attenuation γ shown in Equation 1.1.

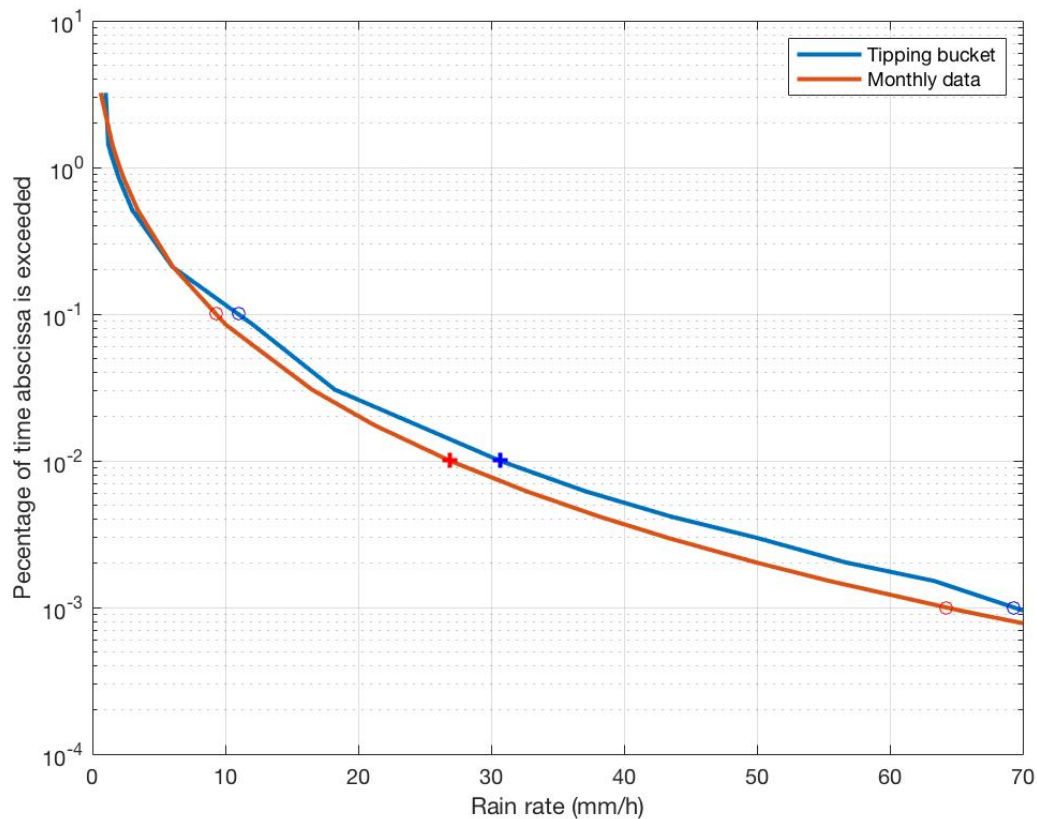


Figure 2.6 Percentage of time and rain rate for Oslo Blindern data using monthly data (Seklima) and tipping bucket data

2.3. Method of deriving rain height

The ERA5 data are assimilated from numerical weather prediction modeling (from ECMWF/Copernicus) and used to calculate a large number of climate data from the year 1950 to 2020 (Bell et al., 2020; Hersbach et al., 2019). The climate data have three dimensions which are longitude latitude and time. In addition to that, it has a source parameter of temperature ($t2m$) in Kelvin which means the temperature of the air 2 meters above the surface, geopotential (z) in m^2/s^2 , and surface air pressure (sp) in Pa.

Finally, it includes the zero-degree isotherm ($deg0l$) in meter. It is the parameter of the height that is taken above the earth's surface where the temperature changes from positive to negative and corresponds to the top of a warm layer at the specified time. Since the temperature above the earth gets colder and colder as it passes through the atmospheric layer.

If there is one more warm layer, a zero-degree level corresponds to the top of the second atmospheric layer. For the negative temperature, the zero-degree isotherm is set to zero. The data from ERA5 is used to derive the rain height and temperature at the surface. Decadal temperature and rain height anomalies are taken for the year 1950-1980 as the reference period.

Rain height is derived from a geometric height that is downloaded from ERA5. Geopotential height (Z) is calculated from the surface geopotential (z) in m^2/s^2 by dividing with gravitational acceleration (g), where $g = 9.80665 m/s^2$ and the radius of the earth $R_e = 6378 \cdot 10^3 m$.

$$Z = \frac{z}{g} \quad 2.1$$

$$h_{geo} = \frac{ZR_e}{R_e - Z} \quad 2.2$$

$$h_o = h_{geo} + deg_{ol} \quad 2.3$$

where (h_{geo}) is geometric height, zero-degree height (h_o). Then rain height (h_R) is calculated by using Equation 1.6.

3. Result of climate parameter analysis

The ERA5 data by ECMWF that are used in the thesis are available at a spatial resolution of 0.25° in longitudes and latitudes and monthly temporal resolution. These data are suitable for the estimation of temperature and rain height, as presented in Chapters 3.1 and 3.2. However, for rain rate, other data must be used as indicated in Chapter 2.2.

3.1. Reference temperature and decadal anomalies

To determine decadal temperature and rainfall height anomalies, the years 1950 to 1979 are used as a reference period. The reference temperature at the surface, i.e., the parameter $t2m$ in the ERA5 dataset, is calculated and illustrated in Figure 3.1, i.e., temperature $T(^{\circ}\text{C}) = t2m + 273.15$.

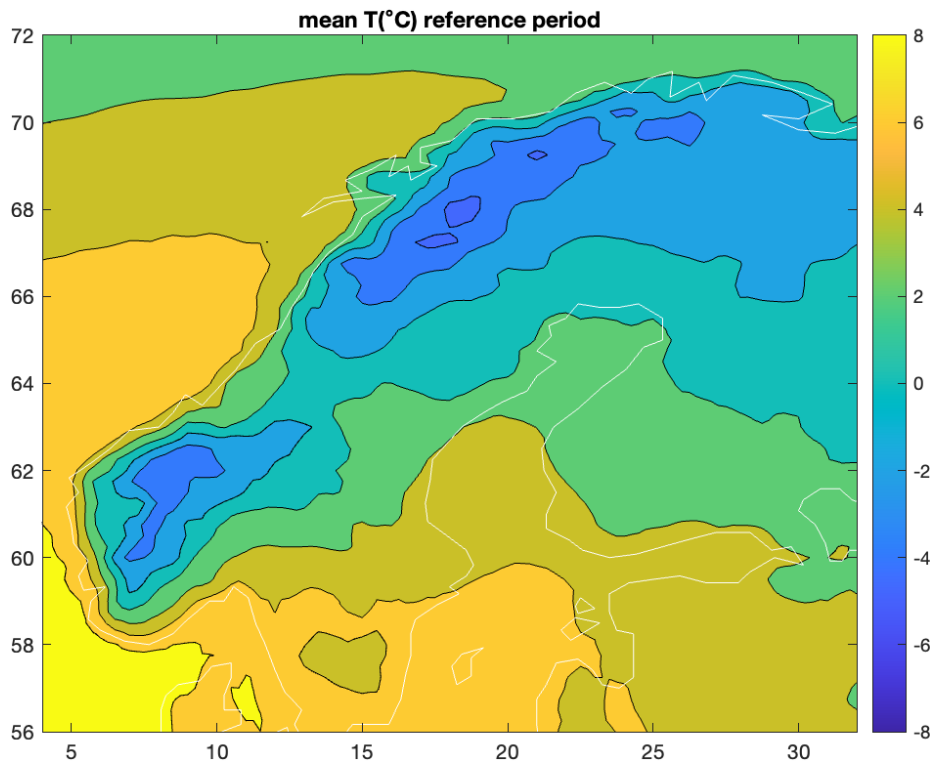


Figure 3.1 Surface temperature for the reference period 1950 to 1979

The mean temperature anomalies shown in Figure 3.2 explain the deviation in four decades, 1950-1959 (50s), 1970-1979 (70s), 1990-1999 (90s), and 2010-2019 (2010s). Figure 3.2a is for the decade from 1950 to 1959 compared with the reference temperature. It has a negative deviation from the reference period as we see from the color. Whereas the decades for 70s, 90s and 2010s in Figure 3.2b, c and d respectively, have shown a positive deviation for some areas as time passes.

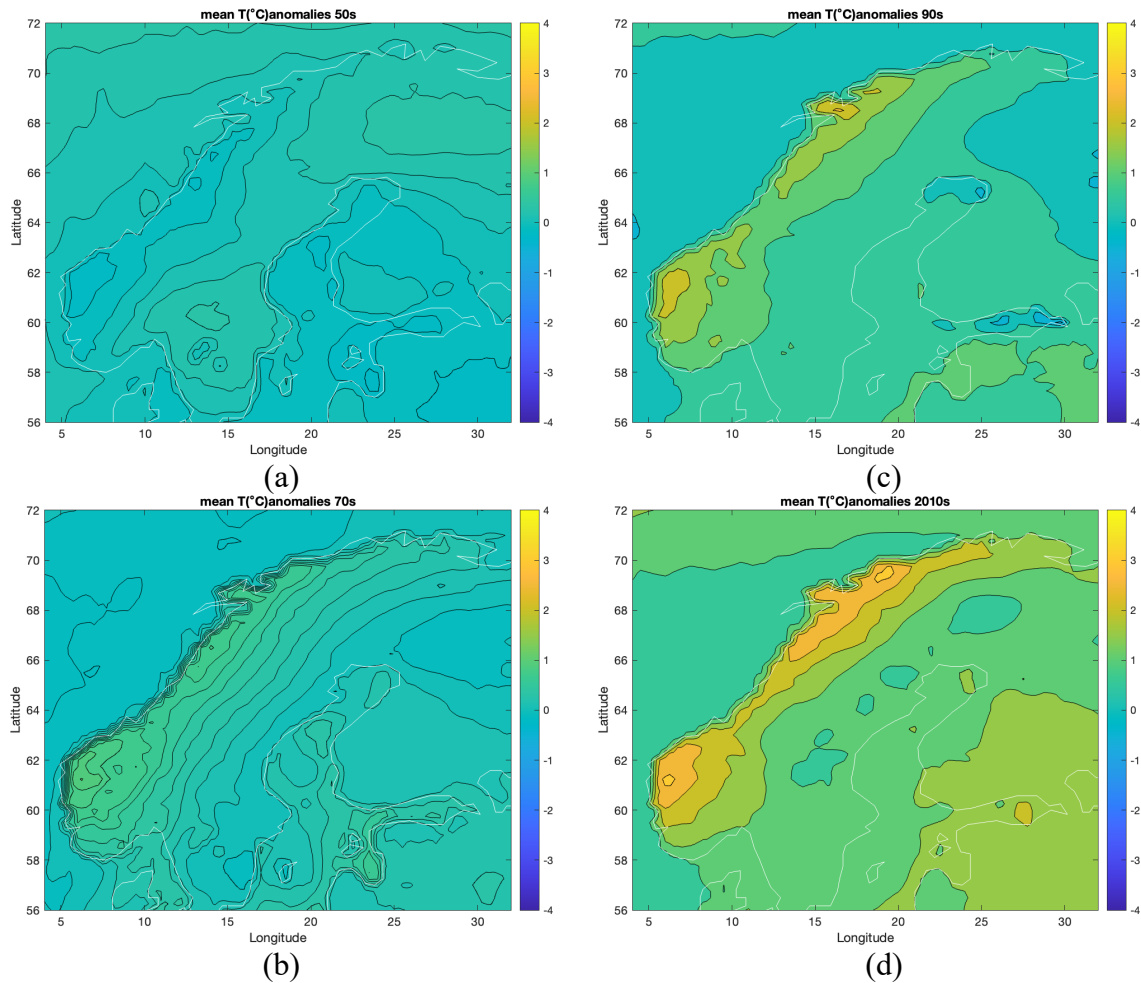


Figure 3.2 Mean decadal temperature anomalies for four decades where (a) is the decade 1950-1959, (b) from year 1970-1079, (c) from year 1990-1999 and (d) from year 2010-2019

The mean temperature anomalies had high variability through the decades. This shows that in southern Norway for certain areas there is an increase of 3°C in the decade 2010-2019 from the reference period. In the lower altitudes, such as coastal areas, the increase is around 1°C, which is more in line with global temperature increases (Morice et al., 2021).

3.2. Reference rain height and decadal anomalies

Rain height in the reference period is calculated as well, from the years 1950 to 1979 is shown in Figure 3.3. It varies from about 1000 m to 2100 m in Norway.

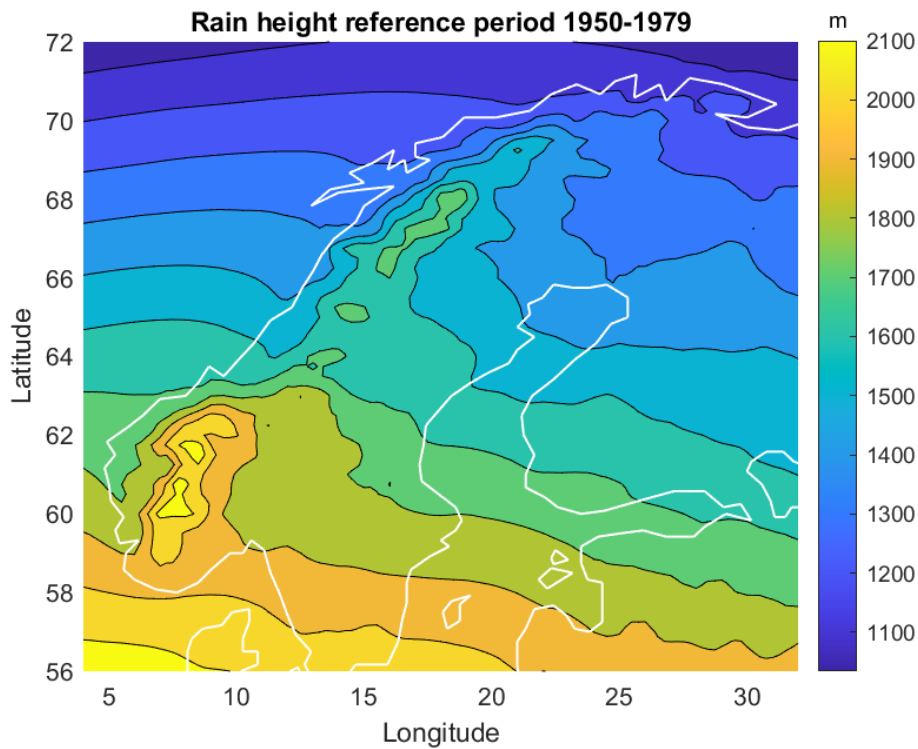


Figure 3.3 Rain height (m) in the reference period

Figure 3.4 shows the decadal anomalies for four decades, 50s, 70s, 90s and 2010s. The decades of 50s and 70s do not show a significant change in Norway, perhaps even a negative trend in the 70s. The decade 90s and 2010s show an increase for certain parts, for the 90s in the southern part of Norway and in 2010s in large parts of the country but apparently not so much in the interior mountainous parts. The mean rain height difference in the 2010s decade increases up to about 200 m in certain. Areas. For the southeast Norwegian coastal area, there seems to be a slightly larger positive deviation compared to northern Norway.

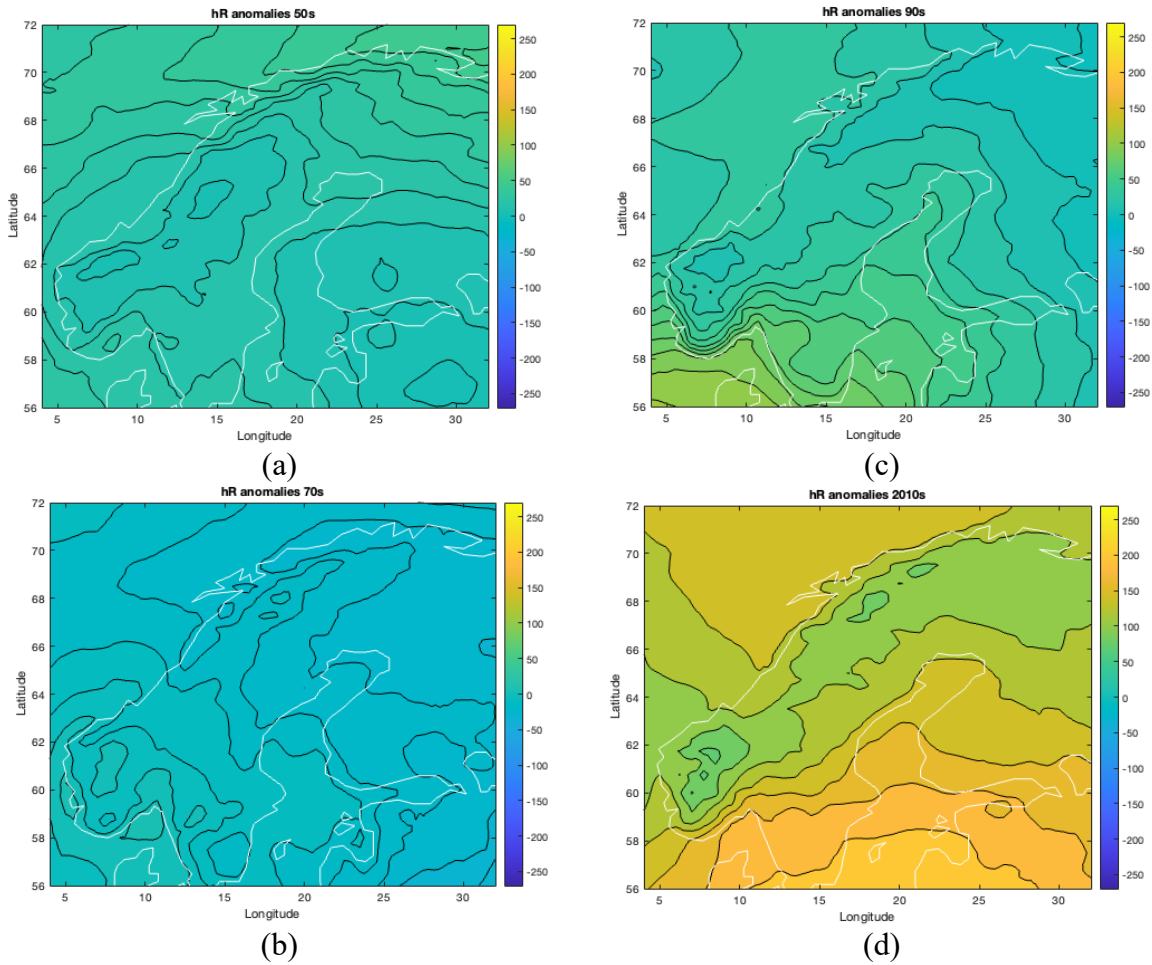


Figure 3.4 Mean decadal rain height anomalies for four decades where (a) is the decade 1950-1959, (b) from year 1970-1079, (c) from year 1990-1999 and (d) from year 2010-2019

A typical temperature lapse rate with height is about 6 to 7°C per 1000 m (Gardner et al., 2009). This means that a 1°C increase in temperature might result in about 140 m to 160 m change of the zero-degree height, and hence the rain height. Apparently, the mountainous areas of Norway showing a significant temperature increase with respect to the reference period, of event 3°C does not show a change in the rain height of this order. In fact, the lapse rate has apparently changed as well.

3.3. Selection of different locations and estimating climate data

The locations that are used to study rain attenuation are shown in Figure 3.5. They are selected to study different locations across Norway. The meteorological stations chosen represent locations that have sufficient data. The station information: station number, longitude, latitude and height are taken from the Seklima database.

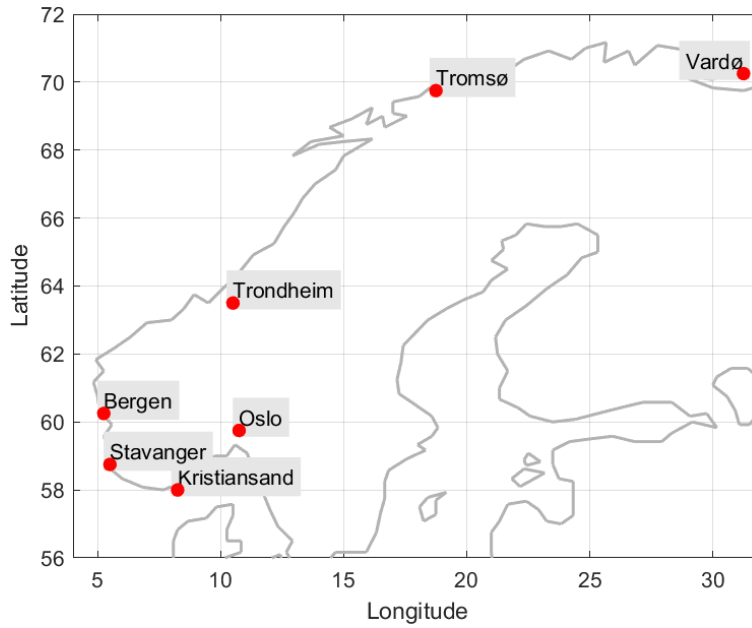


Figure 3.5 Map of the selected location

The information about the selected sites and station names and numbers (SN) are stated in Table 2 and Table 3. The longitude latitude and altitude used in ERA5 data and for the meteorological stations are listed as well in Table 3. In the tipping bucket data, cities such as Bergen and Trondheim have data from the same city but are selected from two or three different stations. The reason of doing that is to take the data from each station which has enough time series in each year for the calculation of rain rate.

Location	Monthly data		Tipping bucket	
	Station	SN	Station	SN
Oslo	Blindern	18700	Blindern	18701
Kristiansand	Kjevik	39040		39150
Stavanger	Sola	44560	Sandnes	44730
Bergen	-	-		50490 & 50480
Trondheim	Værnes	69100		68170, 68230, 68190
Tromsø		90450	-	-
Vardø	Radio	98550	-	-

Table 2 Selected stations name and number

Location	Tipping bucket	Monthly data	Meteorological location			ERA5		
	SN		SN	Longitude	Latitude	Altitude (m)	Longitude	Latitude
Oslo	18701	18700	10.72	59.94	94	10.75	59.75	117.6
Kristiansand	39150	39040	8.08	58.2	12	8.25	58	16.3
Stavanger	44730	44560	5.64	58.88	7	5.5	58.75	5.6
Bergen	50490 50480	-	5.278	60.29	37	5.25	60.25	83.6
Trondheim	68170 68190 68230	69100	10.93	63.46	12	11.63	63.5	278.5
Tromsø	-	90450	18.93	69.65	100	18.75	69.75	176.6
Vardø	-	98550	31.09	70.37	10	31.25	70.25	7.7

Table 3 Locations and list of meteorological stations that are used in the analysis

In general, the meteorological stations are close to each other and have the data for long-term analyses. Then after the selection of grid points in ERA5 the analyses of radio systems are done to calculate rain height (Bell et al., 2020; Hersbach et al., 2019).

The data downloaded from ERA5 are divided into two sources. One is from 1950 to 1978 year and the other one is from 1979 to the present. The two datasets cover precisely the same area and have exactly the same resolution such that we can easily merge the full period from 1950 to 2020. We have taken four grid points as shown in Table 4 surrounding each location and check the best grid points based on the proximity in longitude, latitude and altitude of the selected locations. For example, the station Oslo-Blindern has shown the closest proximity at grid point longitude (gpLon) 10.75, grid point latitude (gpLat) 59.75 and grid point altitude (gpAlt) 117.6. The selected sites with grid points and indexes to find the longitude and latitude (idxLon and idxLat) are marked with an underline in the table.

Station	SN no	Long	Lat	Alt	gpLon	gpLat	gpAlt	idxLon	idxLat
Oslo - Blindern	18700	10.72	59.94	94.0	10.50	60.00	255.5	27	49
					10.50	59.75	146.3	27	50
					10.75	60.00	246.8	28	49
					10.75	59.75	117.6	28	50
Bergen - Sandsli	50480	5.28	60.29	37.0	5.25	60.50	117.0	6	47
					5.25	60.25	83.6	6	48
					5.50	60.50	270.5	7	47
					5.50	60.25	156.8	7	48
Kjeviek	39040	8.08	58.20	12.0	8.00	58.25	151.5	17	56
					8.00	58.00	16.3	17	57
					8.25	58.25	92.0	18	56
Sola	44560	5.64	58.88	7.0	5.50	59.00	-3.7	7	53
					5.50	58.75	5.6	7	54
					5.75	59.00	81.4	8	53
					5.75	58.75	97.6	8	54
Værnes	69100	10.93	63.46	12.0	10.75	63.50	193.1	28	35
					10.75	63.25	359.1	28	36
					11.00	63.50	278.5	29	35
Tromsø	90450	18.94	69.65	100.0	11.00	63.25	445.4	29	36
					18.75	69.75	176.6	60	10
					18.75	69.50	247.2	60	11
					19.00	69.75	211.1	61	10
Vardø Radio	98550	31.10	70.37	10.0	19.00	69.50	296.0	61	11
					31.00	70.50	55.2	109	7
					31.00	70.25	19.5	109	8
					31.25	70.50	13.1	110	7
					31.25	70.25	7.7	110	8

Table 4 Locations with four grid points and selected indexes in ERA5 considered with geographical location taken from monthly data

3.4. System parameters for the terrestrial links and satellite links

The system design is done by defining the terrestrial system that is suitable for connecting mobile network base stations to the backbone network. Such a connection may provide service at 99.995% availability or even more, and the rain attenuation exceeding at 0.005% is therefore of interest. A terrestrial link may typically be designed for up to 40 dB fade margin. The radio frequencies 18 GHz and 38 GHz are commonly used, as is linear horizontal polarization.

Using the data from the selected areas and years around four decades, rain attenuation for a terrestrial link and satellite link is calculated using the prediction method mentioned in Chapter 1. For the design, we have selected a radio link system parameter shown in Table 5 for the terrestrial link. It is designed for two frequencies 18 GHz with a path length of 15 km and 38 GHz with a path length of 4 km. Linear horizontal polarization ($pol = 0$) with rain attenuation exceeding at $p = 0.005\%$ is used.

Terrestrial link				
Location	<i>Freq</i>	<i>path length</i>	<i>pol</i>	<i>p</i>
	(GHz)	(km)	(°)	(%)
Oslo	18	15	0	0.005
	38	4		
Kristiansand	18	15	0	0.005
	38	4		
Stavanger	18	15	0	0.005
	38	4		
Bergen	18	15	0	0.005
	38	4		
Trondheim	18	15	0	0.005
	38	4		
Tromsø	18	15	0	0.005
	38	4		
Vardø	18	15	0	0.005
	38	4		

Table 5 System for terrestrial link

We have also defined a couple of satellite systems, one for a consumer terminal at the Ka-band (20 GHz) and one for a teleport feeder link at the Q/V band (50 GHz) (Maral & Bousquet, 2009; Sizun, 2005). The first would provide an availability of 99.95%, and the second one provides 99.99%. This means up to 10 dB attenuation for the first link, and probably more than 40 dB for the second link. The geostationary satellite is located at -1° East. The parameters chosen for the satellite link are shown Table 6. The frequencies used are 20 GHz and 50 GHz with linear horizontal polarization (deg. 0). The elevation angle used are listed in the table. The station heights are set to the height slightly above the altitudes in ERA5 data.

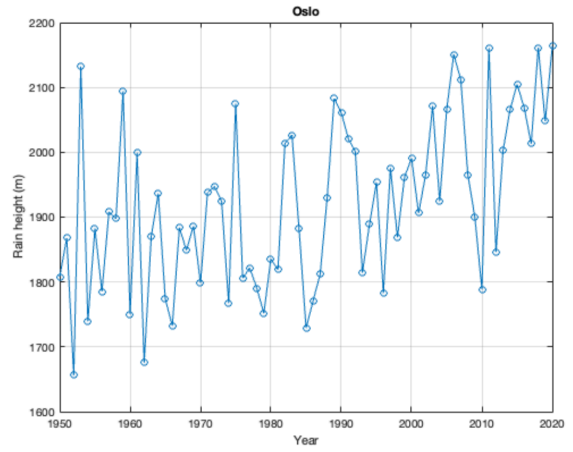
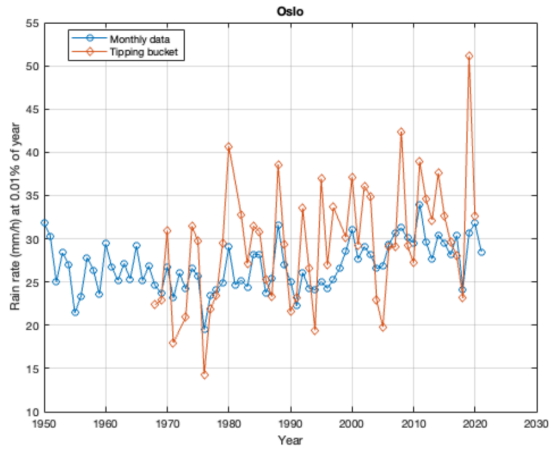
The elevation angles used are listed in the table, and are derived from the station coordinates and the geostationary satellite position.

Satellite link						
Location	<i>Freq.</i>	<i>Elevation angle</i>	<i>polarization</i>	<i>percent</i>	<i>Sat position</i>	<i>hs</i>
	(GHz)	(deg)		(%)		(km)
Oslo	20 50	21.5	0	0.05 0.01	-1	0.12
Kristiansand	20 50	23.3	0	0.05 0.01	-1	0.01
Stavanger	20 50	23	0	0.05 0.01	-1	0.09
Bergen	20 50	21.5	0	0.05 0.01	-1	0.16
Trondheim	20 50	17.6	0	0.05 0.01	-1	0.2
Tromsø	20 50	10.5	0	0.05 0.01	-1	0.18
Vardø	20 50	8.1	0	0.05 0.01	-1	0.01

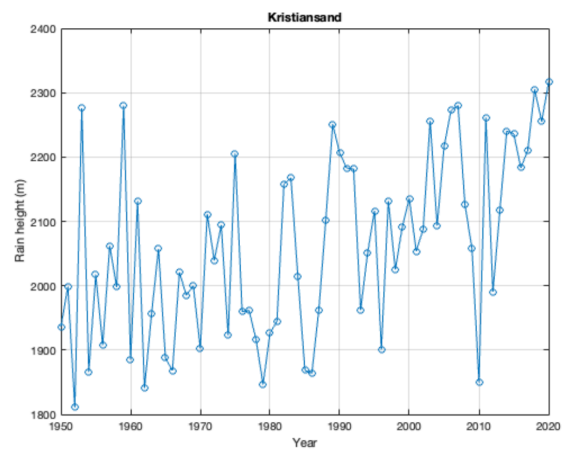
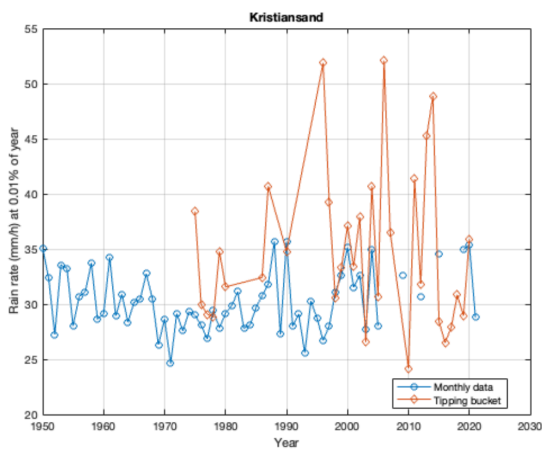
Table 6 System for satellite link

3.5. Rain height and rain rate time series

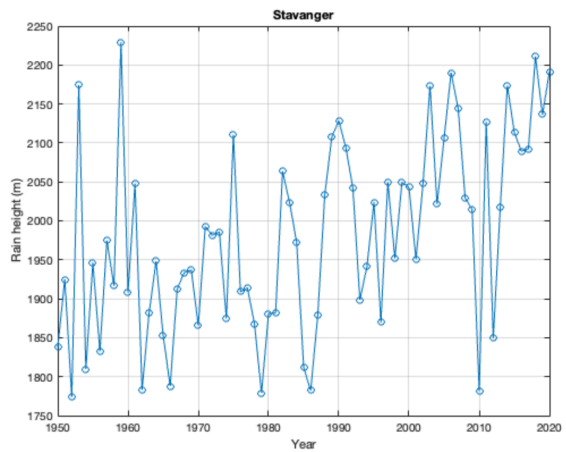
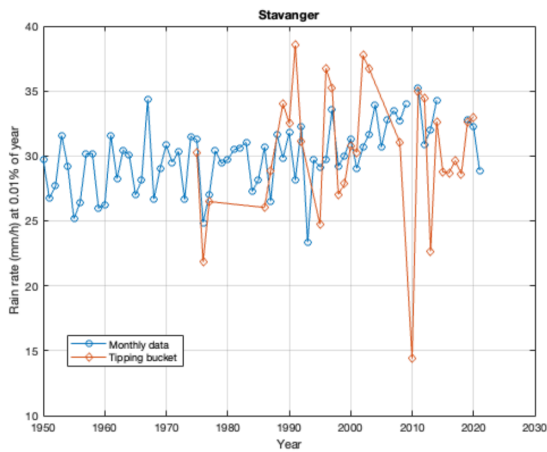
The input parameter rain height and rain rate time series results of the selected locations are shown in Figure 3.6, Figure 3.7 and Figure 3.8. The rain rate results from tipping bucket data and monthly data are both used in further analysis. It shows time series data from 1950 to 2020 for rain rate based on monthly data and the rain height (derived from the ERA5 data) for all locations. The rain rates derived from tipping bucket data start later, from slightly before 1970 or slightly after, depending on the location. Figure 3.6 a, b, c shows the rain rate and rain height time series in Oslo, Kristiansand and Stavanger. We can see the rain height varies a lot but with an increase up to 300m in these areas after 1980. Whereas rain rate from the tipping bucket source has shown a similar trend excluding the years that have shown higher variability. It is apparent that the tipping bucket source results in higher variability than the monthly data source.



(a)



(b)

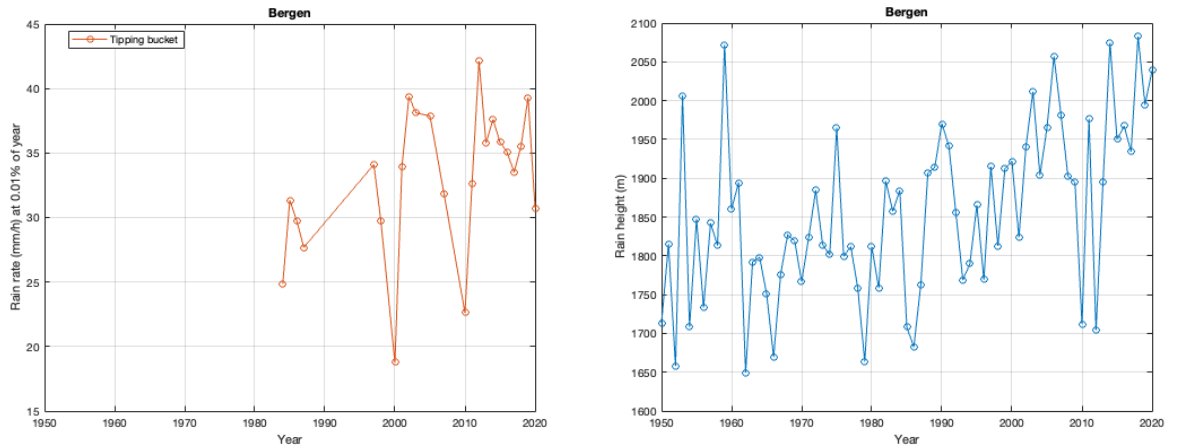


(c)

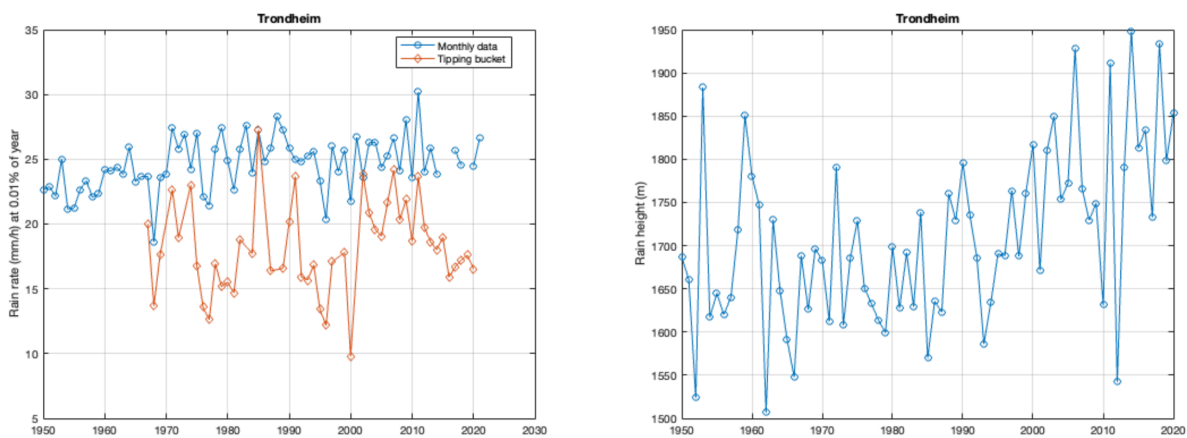
Figure 3.6 Rain height and rain rate time series (a) Oslo, (b) Kristiansand, (c) Stavanger

The rain height and rain rate time series in Bergen and Trondheim are shown in Figure 3.7. Rain height increases between 150 m to 200 m at both sites after 1980. However, the rain rate

from tipping bucket data in Bergen is lacking enough data, and it seems the trend is increasing. The rain rate in Trondheim is uncertain to judge the trend. Since there has been a higher variability from the monthly data. The trend in monthly data is flat means there is no significant change. However, the trend in tipping bucket data is decreasing since the 2000 year.



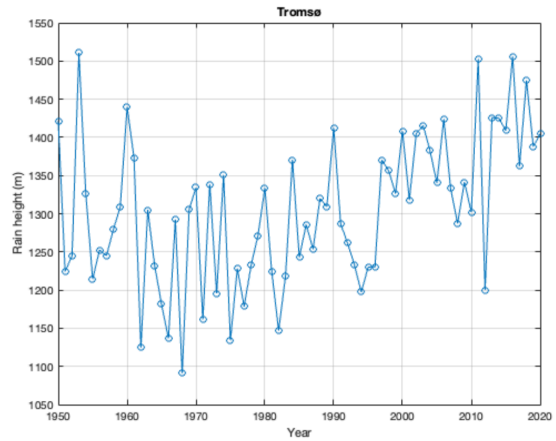
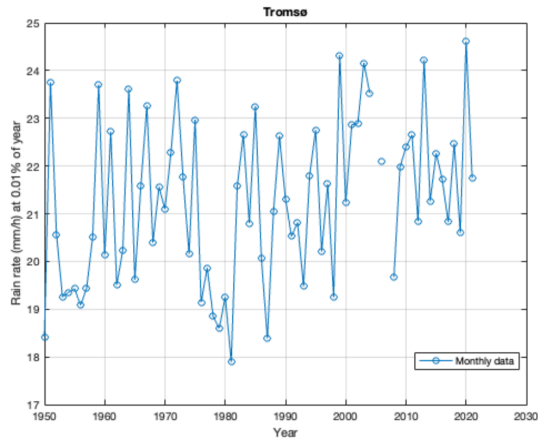
(a)



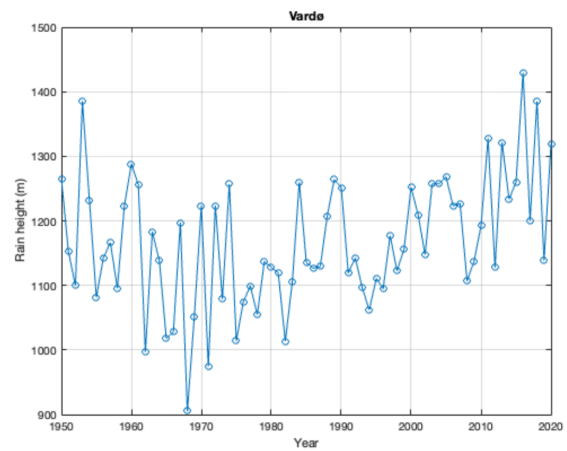
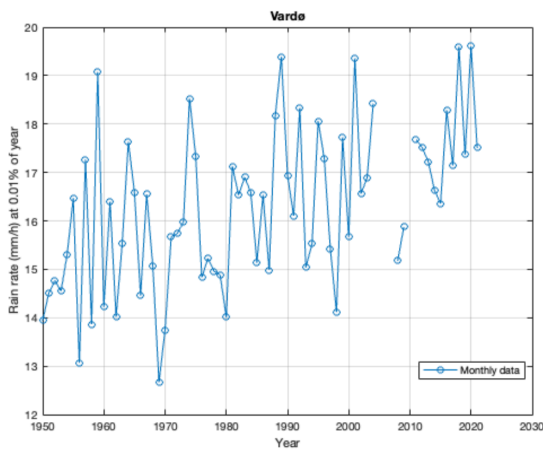
(b)

Figure 3.7 Rain height and rain rate time series (a) Bergen, (b) Trondheim

Similarly, the rain height time series shown in Figure 3.8 for Tromsø and Vardø is increasing after the period of 1980 by approximately 250 m. since we have only the monthly data for rain rate time series and there are few data available between the years 2010 and 2020. It is difficult to say there is an increase in rain height even though we see some changes in Vardø.



(a)



(b)

Figure 3.8 Rain height and rain rate time series (a) Tromsø and (b) Vardø

Overall, we have seen that the rain height increases in all the selected locations in the period 1980 - 2020. That is an increase of up to 300 m in the selected locations. In addition to that, the rainfall rate is increasing in a few areas for this period. As a result of that, we will see a change in rain attenuation in this period. Since rain rate is a common input for both terrestrial and satellite links, whereas rain height is used for satellite link rain attenuation.

3.6. Attenuation time series for terrestrial links and satellite links

It has been noted that it is important to dimension a radio system by choosing suitable climate parameters for a longer period. For that, we have selected four systems in Chapter 3.4 that is two for terrestrial links and two for satellite links. the mean value of the period from 1980 to 2020 is considered for the calculation of rain attenuation since it has shown a significant change in climate parameters for the selected areas.

The rain attenuation methods that are explained in Chapters 1.3 and 1.4 are used to calculate attenuation time series in the period 1950 to 2020. We choose a long-term but recent period when evaluating climate parameters to use for link dimensioning. Therefore 1980 to 2020 is an appropriate choice. We can see that for the location Oslo showed in Figure 3.9 a and b, the terrestrial link and satellite link trend lines are calculated from monthly data and tipping bucket data. In Oslo, there is a similar increment of attenuation trend in all four systems, but attenuation using rain rate derived from monthly data is lower than attenuation from the tipping bucket data.

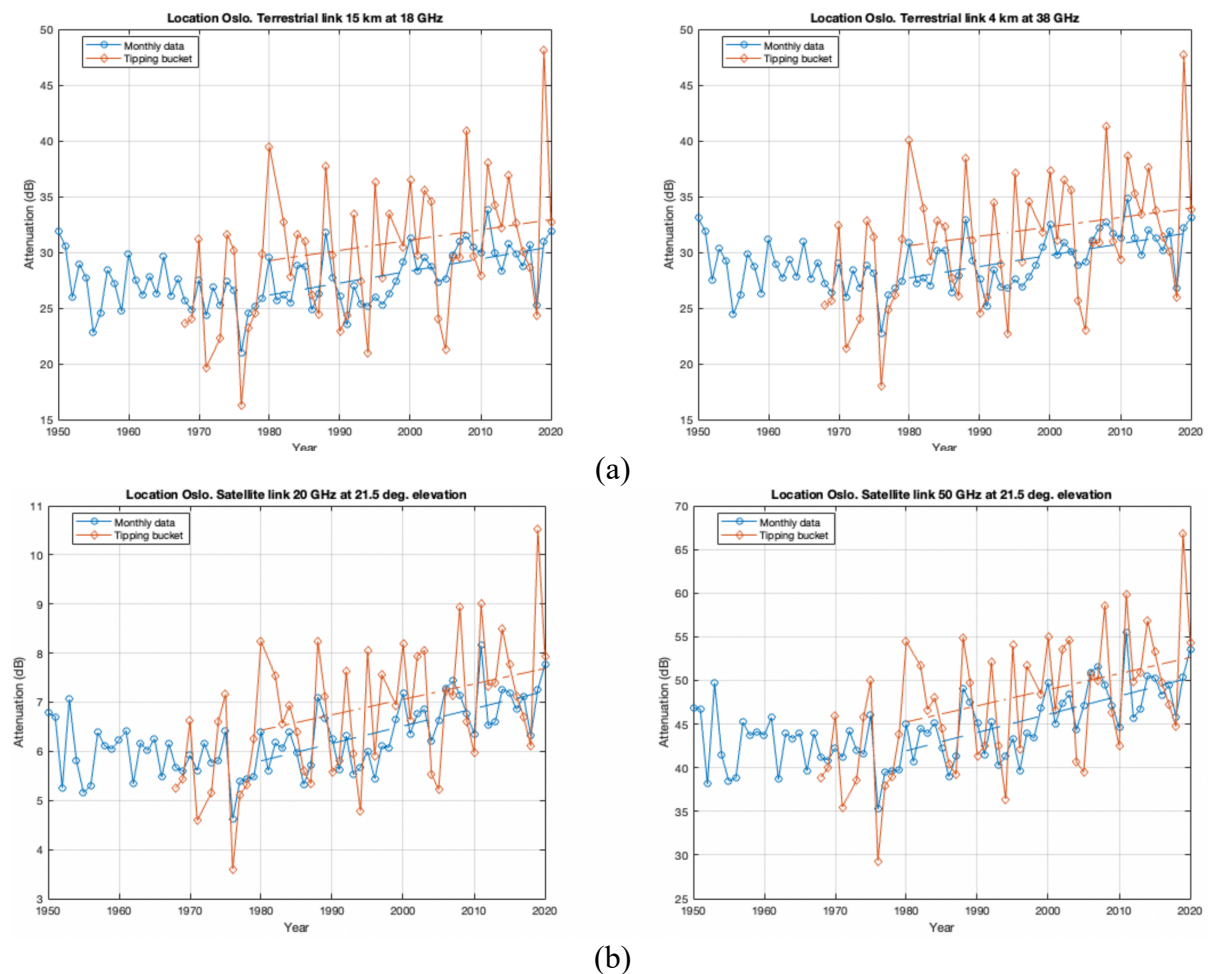


Figure 3.9 Attenuation in Oslo for (a) terrestrial link with frequencies 18 GHz and 38 GHz and (b) satellite link with frequencies 20 GHz and 50 GHz

For the location, Kristiansand shown in Figure 3.10 the attenuation calculated from tipping bucket data has shown a nearly flat trend. Whereas in the monthly data there is an increase in the attenuation trend. There is a similarity between the two systems of satellite links. The rain attenuation increases in the monthly data after the year 1980, is approximately 3 dB in the 20 GHz link and 15 dB in 50 GHz.

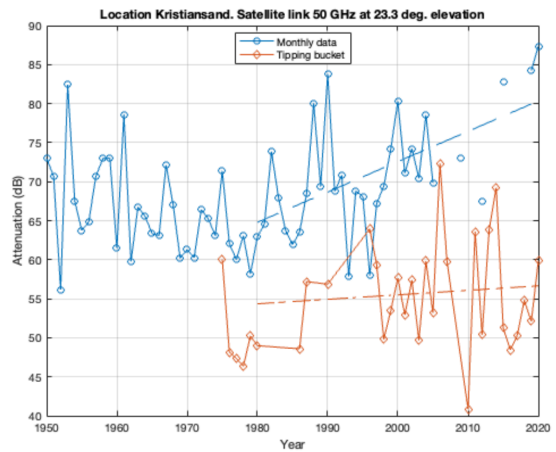
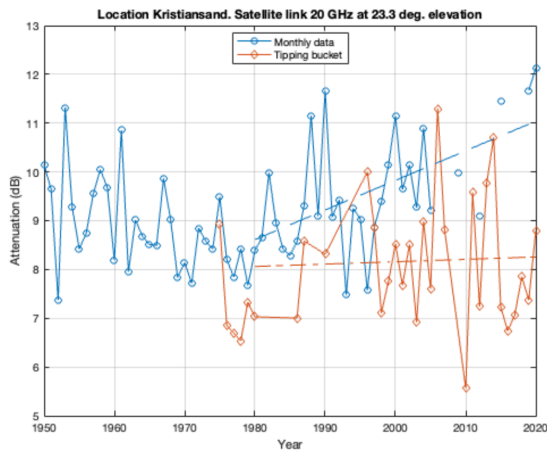
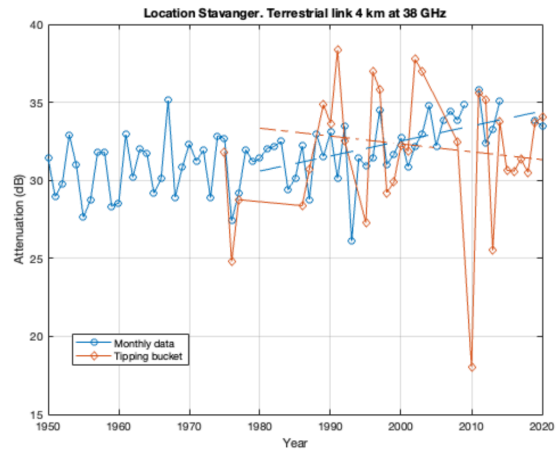
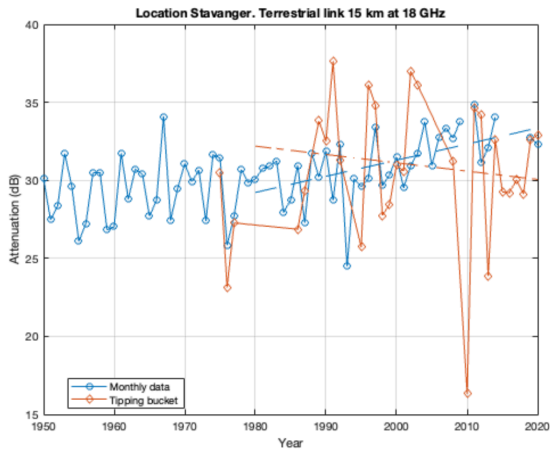
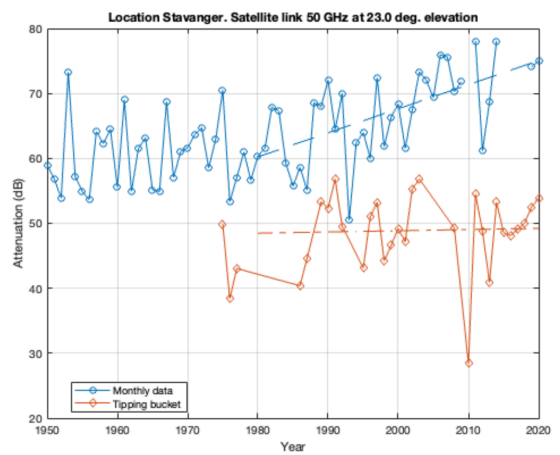
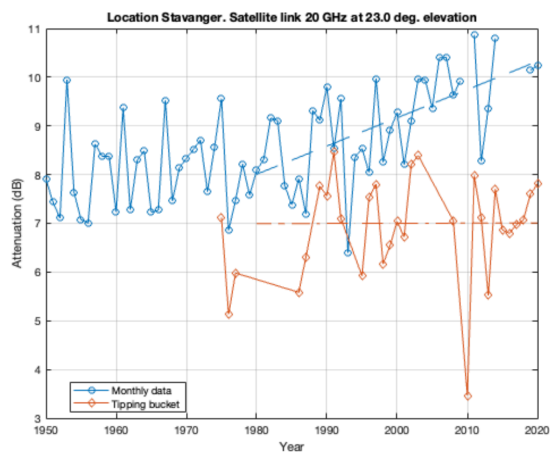


Figure 3.10 Attenuation in Kristiansand for Satellite link with frequencies 20 GHz and 50 GHz

Stavanger city in Figure 3.11 has shown a trend of four systems. It is shown that there is an opposite slope of the rain attenuation trend for both tipping bucket data and monthly data in the terrestrial link. However, the trend in Satellite link tipping bucket data is flat while monthly data is increasing. The rain attenuation increased in the monthly data after the year 1980, which is approximately 4 dB in the 18 GHz link and 4 dB in 38 GHz for the terrestrial link. Likewise, 2 dB in the 20 GHz link and 15 dB in 50 GHz for the satellite link.



(a)



(b)

Figure 3.11 Attenuation in Stavanger for (a) terrestrial link with frequencies 18 GHz and 38 GHz and (b) satellite link with frequencies 20 GHz and 50 GHz

The trend in Bergen has shown a similar increase after the year 1980 for both systems in satellite links. It is shown that about 2 dB increase in 20 GHz and 12 dB increase in 50 GHz system.

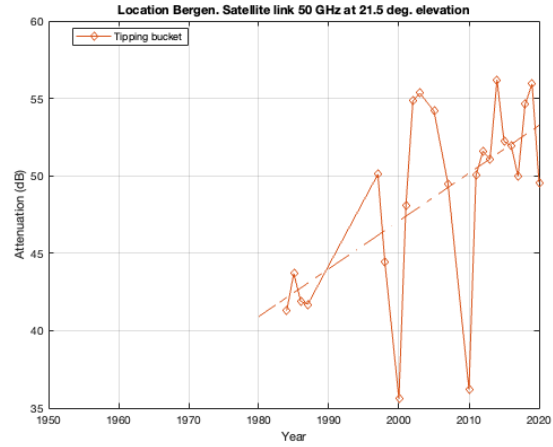
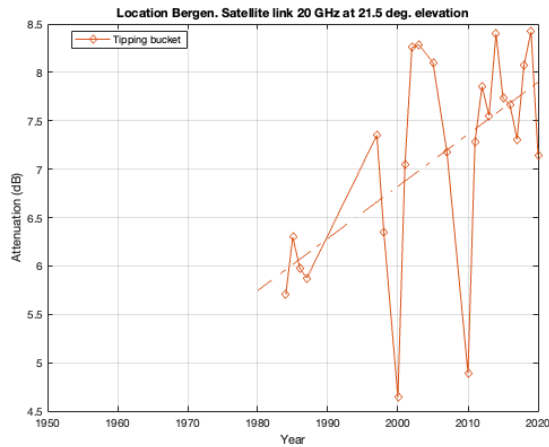
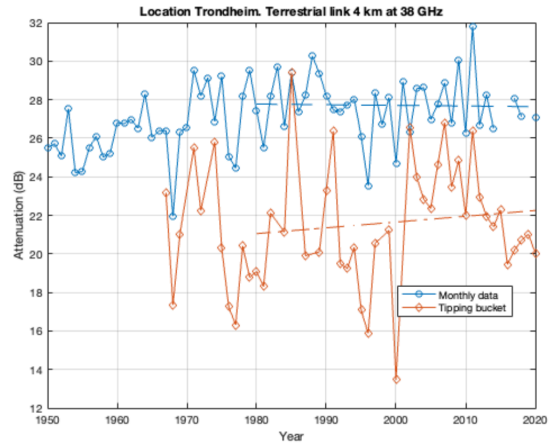
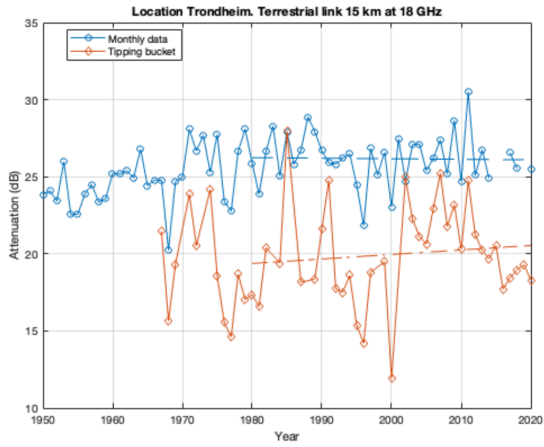
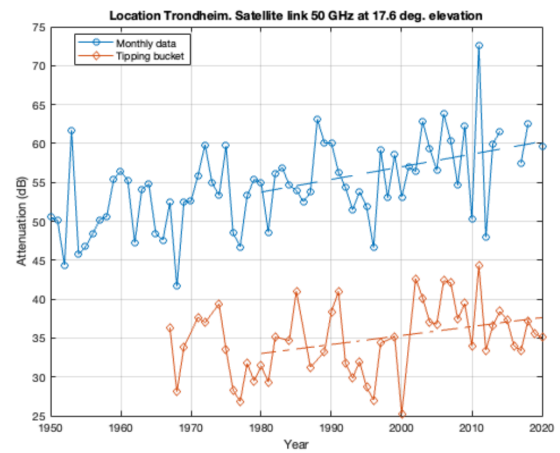
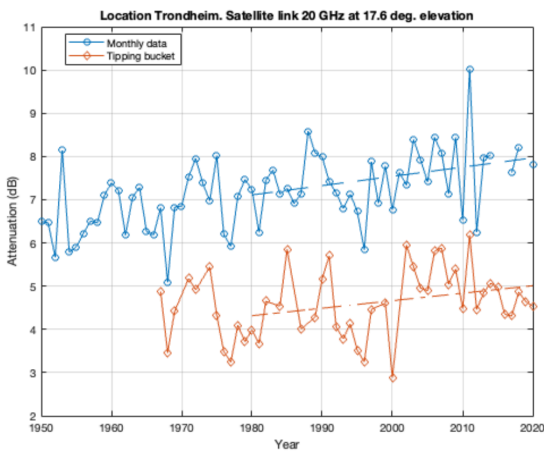


Figure 3. 12 Attenuation in Bergen for satellite link with frequencies 20 GHz and 50 GHz

The trend in Trondheim shown in Figure 3.13 the monthly data is almost flat in both systems of terrestrial links. Moreover, is a slight increase which is around 1dB attenuation trend is shown in tipping bucket data. However, the trends of the two satellite links are increasing apparently. Therefore, it has shown a similarity of increment in both sources.



(a)



(b)

Figure 3.13 Attenuation in Trondheim for (a) terrestrial link with frequencies 18 GHz and 38 GHz and (b) satellite link with frequencies 20 GHz and 50 GHz

Similarly, the trend in Tromsø and Vardø for satellite link shown in Figure 3.14 and Figure 3.15 increased significantly. There is an increase of 1.5 to 2 dB in 20 GHz links and 13 to 15 dB increment shown in 50 GHz in both sites.

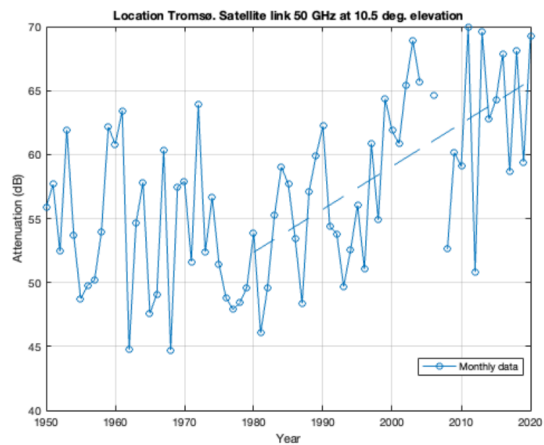
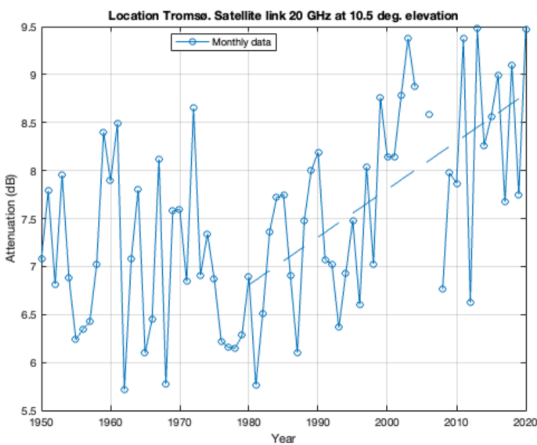


Figure 3.14 Attenuation in Tromsø for satellite link with frequencies 20 GHz and 50 GHz

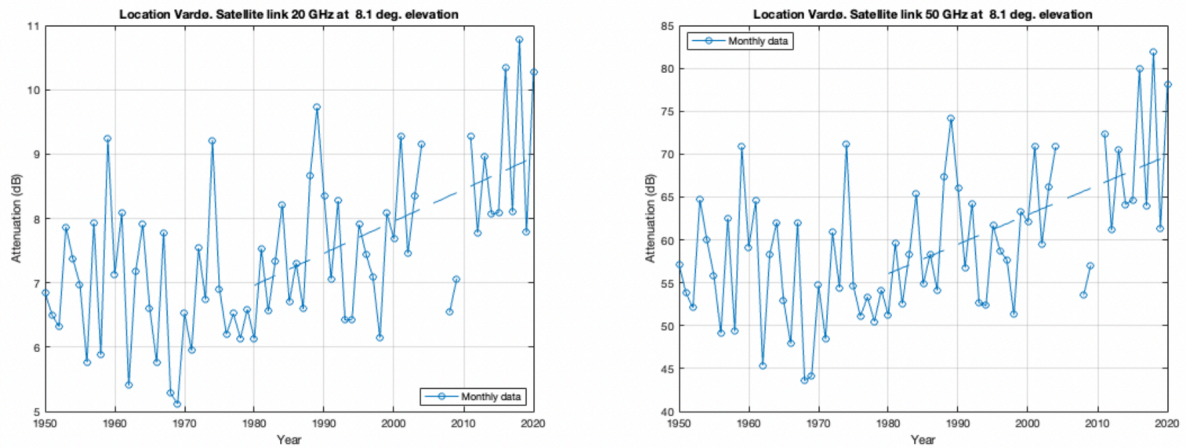


Figure 3.15 Attenuation in Vardø for satellite link with frequencies 20 GHz and 50 GHz

When dimensioning a radio system typical values of rain rate and rain height will be used. For the calculations here we use the value for 2000, which is in the middle of the period 1980 and 2020. Trends of climate input parameters are not used in the dimensioning normally. Dimensioning may take year-to-year variability into account, but not including trends may therefore result in poor dimensioning if the climate input variable increases with time

The attenuation in the middle of the period between 1980 and 2020 is listed in Table 7 for a terrestrial link. We can see that the calculated attenuation using the tipping bucket data shown in this table has different trend coefficients in three locations with a positive value and in two locations with a negative value. And also, the confidence intervals include zero for all of the systems except the one from Bergen. This has shown a static insignificant result and it is difficult to trust the trend.

Comparing the middle period attenuation, which is in year 2020, the monthly data in Oslo and Kristiansand have higher attenuation than tipping bucket data. Stavanger has a very similar attenuation, but Trondheim has shown a larger deviation.

		Terrestrial link attenuation trend calculated using					
	Freq	rain rate from tipping bucket			rain rate from monthly data		
Location	(GHz)	Attenuation (dB) (year 2000)	Trend Coefficient	Confidence interval	Attenuation (dB) (year 2000)	Trend Coefficient	Confidence interval
Oslo	18	31.1	0.0918	-0.07, 0.25	28.3	0.1082	0.05, 0.16
	38	32.3	0.0844	-0.06, 0.23	29.7	0.1020	0.05, 0.15
Kristiansand	18	35.4	-0.0820	-0.32, 0.16	31.4	0.1001	0.02, 0.18
	38	36.3	-0.0765	-0.3, 0.14	32.6	0.0928	0.02, 0.17
Stavanger	18	31.1	-0.0533	-0.22, 0.12	31.3	0.1033	0.05, 0.16
	38	32.3	-0.0502	-0.21, 0.11	32.5	0.0961	0.046, 0.15
Bergen	18	31.9	0.1871	0.01, 0.36			
	38	33	0.1735	0.012, 0.34			
Trondheim	18	20	0.0293	-0.06, 0.12	26.2	-0.0035	-0.05, 0.04
	38	21.7	0.0299	-0.06, 0.12	27.7	-0.0034	-0.05, 0.04
Tromsø	18				22.9	0.0455	0.01, 0.08
	38				24.6	0.0443	0.01, 0.08
Vardø	18				18.7	0.0383	0.004, 0.07
	38				20.4	0.0383	0.004, 0.07

Table 7 Rain attenuation trend coefficients and confidence intervals in terrestrial links

The attenuation in the middle of the year between 1980 and 2020 is listed in Table 8 for the satellite link. We can also see that the tipping bucket data has shown different trend coefficients with negative coefficients for two locations and positive coefficients for three locations. Whereas the confidence interval includes zero except for Bergen. This has shown a

statical insignificant result and there is no attenuation change. The attenuation based on monthly data for Trondheim is not showing a trusted trend as well.

The monthly trend in Oslo, Kristiansand, Stavanger and Trondheim has approximately (1 dB, 2 dB, 2 dB and 3 dB) difference from the tipping bucket trend in 20 GHz link. Additionally, the monthly trend in Oslo, Kristiansand, Stavanger and Trondheim has approximately (3 dB, 8 dB, 18 dB and 22 dB) differences from the tipping bucket trend in 50 GHz link.

		Satellite link attenuation trend calculated using					
	Freq	rain rate from tipping bucket			rain rate from monthly data		
Location	(GHz)	Attenuation (dB) (year 2000)	Trend Coefficient	Confidence interval	Attenuation (dB) (year 2000)	Trend Coefficient	Confidence interval
Oslo	20	7.1	0.0314	-0.001, 0.06	6.5	0.0354	0.02, 0.05
	50	48.9	0.1844	0.012, 0.36	46.1	0.2090	0.13, 0.29
Kristiansand	20	8.2	0.0049	-0.045, 0.055	9.8	0.0607	0.03, 0.1
	50	55.5	0.0575	-0.21, 0.32	72.6	0.3887	0.18, 0.60
Stavanger	20	7	0.0003	-0.04, 0.04	9.2	0.0579	0.03, 0.08
	50	48.9	0.0184	-0.21, 0.25	67.6	0.3705	0.2, 0.54
Bergen	20	6.8	0.0538	0.018, 0.09			
	50	47.1	0.3087	0.11, 0.5			
Trondheim	20	4.7	0.0173	-0.005, 0.04	7.5	0.0214	-0.001, 0.04
	50	35.3	0.1156	-0.01, 0.24	57	0.1622	0.02, 0.30
Tromsø	20				7.8	0.0497	0.03, 0.07
	50				59.1	0.3355	0.2, 0.48
Vardø	20				8	0.0496	0.02, 0.08
	50				62.9	0.3434	0.15, 0.53

Table 8 Rain attenuation trend coefficients and confidence intervals for satellite links

4. Discussion of rain analysis and future work

Designing a radio link, it is essential to evaluate long-term climate parameters data for the location where the link shall operate. We need to consider the link availability and calculate rain attenuation to secure that the system satisfies the wanted requirements. For example, to operate at 99.995% availability of an average year.

4.1. Rain attenuation in terrestrial links

We have designed two systems for a terrestrial link in Chapter 3.4 that operate at 99.995% availability of an average year. Table 9 shows the rain attenuation trend change over four decades for the terrestrial systems. The terrestrial system climate parameter concerning rain attenuation is only the rain rate. The trend depends on whether the rain rate is derived from tipping bucket data or from monthly data. If the rain rate is derived from monthly data all locations show a rain attenuation increase for both terrestrial systems, except for Trondheim. Here the trend is slightly negative, but the trend coefficient is not statistically confident at a 5% confidence level used to estimate the confidence interval, see Table 7. If the rain rate is derived from tipping bucket data, there is only a positive trend line for Bergen. At all other locations, the terrestrial rain attenuation trend line coefficients are small, and they are not statically significant, see Table 7.

The tipping bucket data are direct measurements of the rain rate, while the rain rate derived from monthly data is an indirect method. This may raise a question of the indirect method validity. Also missing year of data, mostly of the tipping bucket data time series, may lead to a less certain estimate of the trend line. In the period studied, 1980 to 2020, there are in general more years missing on tipping bucket data for the locations with monthly data available. For Bergen only tipping bucket data are present, and there are fairly few years of accepted data before 2000 which might suggest less trust in the trend line calculated, although it is statically significant. For Trondheim, it should be noted that the distance between the tipping bucket measurement site and the monthly data measurement site is in the order of 26 km. Location differences cannot perhaps be ignored and may explain the difference in rain rate and hence rain attenuation for Trondheim.

Overall, we have seen an increase in attenuation in Oslo, Bergen, Tromsø and Vardø in four decades. Oslo and Kristiansand have nearly the same attenuation trend value in 2020 in both sources of rain rate data.

Terrestrial link								
	Freq	path length	Pol.	p	Tipping bucket		Monthly data	
Location	(GHz)	(km)		(%)	Attenuation (dB) in 2020	Increase in 4 decades (dB)	Attenuation (dB) in 2020	Increase in 4 decades (dB)
Oslo	18	15	0	0.005	32.93	3.68	30.49	4.33
	38	4	0	0.005	33.97	2.75	31.78	4.08
Kristiansand	18	15	0	0.005	34.73	-3.06	34.49	3.72
	38	4	0	0.005	33.77	-3.28	33.41	4
Stavanger	18	15	0	0.005	30.06	-2.13	33.35	4.13
	38	4	0	0.005	31.33	-2.01	34.44	3.84
Bergen	18	15	0	0.005	36.49	6.94		
	38	4	0	0.005	36.62	7.49		
Trondheim	18	15	0	0.005	20.54	1.17	26.1	-0.14
	38	4	0	0.005	22.25	1.2	27.6	-0.13
Tromsø	18	15	0	0.005			23.84	1.77
	38	4	0	0.005			25.47	1.83
Vardø	18	15	0	0.005			19.44	1.54
	38	4	0	0.005			21.16	1.86

Table 9 Terrestrial link rain attenuation change in four decades

4.2. Rain attenuation satellite links

Similarly, we have proposed two systems for a satellite link in Chapter 3.4 with 99.95% and 99.99% annual availability, respectively. The change in rain attenuation trend over four decades for satellite systems is illustrated in Table 10. The satellite system climate parameters concerning rain attenuation are rain rate and rain height. Using rain rate obtained from monthly data, all locations illustrate an increase in rain attenuation for both satellite systems. The trend is also positive for Trondheim. However, here the trend coefficient is not statistically significant for 20 GHz system. see Table 8. Similarly, using the rain rate derived from tipping bucket data there is only a confident positive trend line for Bergen. At all other locations, the satellite rain attenuation trend line coefficients are small, and they are not statically significant

Similarly, the rain attenuation changes in Table 10 have shown a significant increase in rain attenuation trend in all the monthly data except in Stavanger and Trondheim which has shown a slight small increase in four decades. Furthermore, the cities Kristiansand Stavanger and Trondheim have shown a huge trend difference in attenuation calculation taken from tipping bucket data and monthly data. Hence the attenuation in both sources has shown an increase from 0 dB to 15.55 dB in four decades.

Satellite link										
	Freq	elev angle	Pol.	p	Satp	h_s	Tipping bucket		Monthly data	
	(GHz)	(°)		(%)		(km)	Attenuation (dB) in 2020	Increase in 4 decades (dB)	Attenuation (dB) in 2020	Increase in 4 decades (dB)
Oslo	20	21.5	0	0.05	-1	0.12	7.68	1.25	7.22	1.42
	50	21.5	0	0.01	-1	0.12	52.62	8.38	50.3	8.36
Kristiansand	20	23.3	0	0.05	-1	0.01	8.26	0.2	11.04	2.43
	50	23.3	0	0.01	-1	0.01	56.65	2.3	80.34	15.55
Stavanger	20	23	0	0.05	-1	0.09	7.01	0.01	10.32	2.33
	50	23	0	0.01	-1	0.09	75.05	0.73	49.2	14.8
Bergen	20	21.5	0	0.05	-1	0.16	7.9	2.15		
	50	21.5	0	0.01	-1	0.16	53.26	12.35		
Trondheim	20	17.6	0	0.05	-1	0.2	5.01	0.69	7.97	0.86
	50	17.6	0	0.01	-1	0.2	37.6	4.62	60.25	6.49
Tromsø	20	10.5	0	0.05	-1	0.18			8.8	1.09
	50	10.5	0	0.01	-1	0.18			65.79	13.4
Vardø	20	8.1	0	0.05	-1	0.01			8.95	1.98
	50	8.1	0	0.01	-1	0.01			69.8	13.7

Table 10 Satellite link rain attenuation change in the past 4 decades

Moreover, attenuation approaching 50 dB is more hard to manage with realistic system components. However, it is anyway important to see how heavy rain attenuation could worsen. Site diversity is normally used for this type of system due to the teleports requiring high service availability, and there will always be another hot standby earth station nearby,

often with a large enough distance to improve diversity because rain varies spatially (as well as temporarily).

4.3. Attenuation trend line overview

The summary of the attenuation trend described in Chapter 4.1 and Chapter 4.2 is listed in Table 11 for the terrestrial link. The attenuation trend that is calculated from tipping bucket data increased in four decades except in Kristiansand and Stavanger. However, the trend is not statistically significant (not confident) in all the locations except Bergen. Whereas the attenuation calculated from monthly data increases with a confident trend line, except in Trondheim and the trend is not statically significant.












Terrestrial link 1, 2	Rain attenuation calculated from			
	rain rate tipping bucket		rain rate monthly data	
	Trend direction	Statistically significant	Trend direction	Statistically significant
Oslo		No		Yes
Kristiansand		No		Yes
Stavanger		No		Yes
Bergen		Yes		
Trondheim		No		No
Tromsø				Yes
Vardø				Yes

Table 11 Attenuation trend line overview in terrestrial link

In contrary, the attenuation trend that is listed in Table 12 for the satellite link shows the attenuation calculated from tipping bucket and monthly data increased in all locations for four decades. However, the trend is not statistically significant in all the locations except Bergen. The attenuation calculated from monthly data is increasing and the trend is statistically significant in all locations except the 20 GHz link in Trondheim.













Satellite link 1, 2	Rain attenuation calculated from			
	rain rate tipping bucket		rain rate monthly data	
	Trend direction	Statistically significant	Trend direction	Statistically significant
Oslo		No		Yes
Kristiansand		No		Yes
Stavanger		No		Yes
Bergen		Yes		
Trondheim		No	 , 	No, Yes
Tromsø				Yes
Vardø				Yes

Table 12 Attenuation trend line overview in the satellite link

4.4. Suggested future work

We have selected seven locations in Norway to see the climate change effect on rain attenuation. However, due to short timing, we could not say confidently whether there is attenuation change in the last four decades for a terrestrial link, where there are tipping bucket data used to decide for rain rate. Even though we have seen the effect in some of the selected locations except cities like Trondheim, Stavanger and Kristiansand which have shown opposite results. It might be problematic to have a different result from both sources therefore it requires additional research. In addition, I would suggest modifying the link parameter and checking the effects on attenuation. Moreover, I would suggest selecting more locations that are close to the selected locations and checking the trend is giving a better result.

5. Conclusion

The thesis has analyzed climate parameters needed to estimate radio link rain attenuation variation over the period 1950 to 2020. The trend analysis is done for the four last decades from 1980 to 2020. And it is performed by utilizing two terrestrial link systems and two satellite link systems. Rain attenuation is estimated using ITU-R recommendation methods for terrestrial and satellite links, respectively. The analyses use these four systems placed at seven different locations in Norway: Oslo, Kristiansand, Stavanger, Bergen, Trondheim, Tromsø, and Vardø.

The trend line analyses have been done on the result attenuation distribution for each terrestrial link system for typical values of rain attenuation allocated to the unavailable time. The chosen systems are such that it is not appropriate to compare changes in radio frequency, path length, elevation angle, or the indicated unavailable percentages. However, the change in rain attenuation over the four decades can be compared per system. Utilizing rain rate derived from monthly data all locations have a positive and confident trend line at a 5% confidence level, except at Trondheim. In contrast, if the rain rate is based on tipping bucket data it is only at Bergen there has a confident positive trend line. It should be noted that in this case, the time series input data lack 2/3 of the years before 2000 and this might influence the derivation of the rain rate trend and weaken the certainty of the conclusion. When rain rate is derived by monthly data there are results, for all selected locations, except Bergen. In the terrestrial 18 GHz, 15 km link, the rain attenuation increase is highest in the southern part of Norway, about 5 dB and lowest, even negative in Trondheim, but 1.5 to 2 dB in the northern part. In the terrestrial 38 GHz, 4 km link, rain attenuation increase is about 4 dB in the southern part, 1.3 to 2 dB in the northern part, and Trondheim with no statistically significant trend.

The trend analyses of rain attenuation based on rain rate derived from monthly for 20 GHz satellite link system, show positive and confident coefficients at all locations, except Trondheim. Here the coefficient is not confident. If rain rate is based on tipping bucket data, the trend line is confident only at Bergen. From the monthly data at lower elevation angle (with increasing latitude), rain attenuation increases by about 1 to 2 dB and in a higher elevation angle rain attenuation increases to 2.3 to 2.4 dB.

For the 50 GHz satellite link system, the picture is slightly different. All location's results have positive and confident trend lines if the rain rate is derived from monthly data. However, if rain rate is derived from tipping bucket data this system shows confident trend lines at Oslo and Bergen. In any case, the attenuation for this system is excessive and it will anyway be protected by site diversity. Still, the unavailable time will increase for the protected system as well when the trend line is positive. From the monthly data at lower elevation angle, rain attenuation increases from 8 to 13.7 dB and at higher elevation increases from 14.8 to 15.55 dB.

6. Reference

- Bell, B., Hersbach, H., Berrisford, P., Dahlgren, P., Horányi, A., Muñoz Sabater, J., Nicolas, J., Radu, R., Schepers, D., & Simmons, A. (2020). *ERA5 monthly averaged data on single levels from 1950 to 1978 (preliminary version), copernicus climate change service (C3S) climate data store (CDS)*. Retrieved December 2021 from <https://cds.climate.copernicus.eu/#!/search?text=era5>
- Freeman, R. L. (2006). *Radio system design for telecommunications*. John Wiley & Sons.
- Gardner, A. S., Sharp, M. J., Koerner, R. M., Labine, C., Boon, S., Marshall, S. J., Burgess, D. O., & Lewis, D. (2009). Near-Surface Temperature Lapse Rates over Arctic Glaciers and Their Implications for Temperature Downscaling. *Journal of climate*, 22(16), 4281-4298. <https://doi.org/10.1175/2009JCLI2845.1>
- Hersbach, H., Bell, B., Berrisford, P., Biavati, G., Horányi, A., Muñoz Sabater, J., Nicolas, J., Peubey, C., Radu, R., & Rozum, I. (2019). *ERA5 monthly averaged data on single levels from 1979 to present, Copernicus Climate Change Service (C3S) Climate Data Store (CDS)*. Retrieved December 2021 from <https://cds.climate.copernicus.eu/#!/search?text=era5>
- Hunsperger, R. G. (1995). *Integrated optics* (Vol. 4). Springer.
- ITU-R. (2005). ITU-R recommendations : P.838-3: Specific attenuation model for rain for use in prediction methods P.838-3.
- ITU-R. (2013). Rain height model for prediction methods. *International Telecommunication Union P.Series, Geneva, P839-4*.
- ITU-R. (2017a). Characteristics of precipitation for propagation modelling. *Recommendation ITU-R P.Series, P.837-7*.
- ITU-R. (2017b). ITU-R recommendations : P.618-13 : Propagation data and prediction methods required for the design of Earth-space telecommunication systems P.618-13.
- ITU-R. (2020). Concerning the rainfall rate model given in Annex 1 to Recommendation ITU-R P. 837-7. *Fascicle, Radiocommunication Study Groups working party 3J, Revision 2 to Document 3J/FAS/3-E*.
- ITU-R. (2021). Propagation data and prediction methods required for the design of terrestrial line-of-sight systems. *Recommendation ITU-R P.Series, 530-18*.
- Jeannin, N., Castanet, L., & Lacoste, F. (2013). Model for monthly rainfall rate distribution based on monthly rain amount and average temperature. Joint 19th Ka and Broadband Communications, Navigation and Earth Observation Conference-31st AIAA International Communications Satellite System Conference (ICSSC),
- Kim, J. S., Shin, J. S., Oh, S.-M., Park, A.-S., & Chung, M. Y. (2014). System coverage and capacity analysis on millimeter-wave band for 5G mobile

- communication systems with massive antenna structure. *International Journal of Antennas and Propagation*, 2014.
- Loubere, P. A. (2021). *A History of Communication Technology*. Routledge.
- Mamen, J., & Tjelta, T. (2013). New Norwegian hydrometeor precipitation rate maps derived from long term measurements. 2013 7th European Conference on Antennas and Propagation (EuCAP),
- Maral, G., & Bousquet, M. (2009). *Satellite communications systems : systems, techniques, and technology* (5th ed.). Wiley.
- MET. (2022). *Norwegian center for climate service*. Retrieved April 2022 from <https://www.seklima.met.no>
- Olsen, R. L., Rogers, D. V., & Hodge, D. B. (1978). The a times R to the b relation in the calculation of rain attenuation (rain rate, signal frequency, rain temperature and drop size relations). *IEEE transactions on antennas and propagation*, AP-26, 318-329.
- Sizun, H. (2005). *Radio Wave Propagation for Telecommunication Applications* (1st 2005. ed.). Springer Berlin Heidelberg : Imprint: Springer.
- Sklar, B. (2021). *Digital communications : fundamentals and applications* (Second Edition ed.). Prentice-Hall PTR.
- Tjelta, T., & Mamen, J. (2014). Climate trends and variability of rain rate derived from long-term measurements in Norway. *Radio Science*, 49(9), 788-797.

Annex

Examples of codes used for the analysis

```
% Temperature and Rain height anomalies ERA5
clear all
%ERA5 monthly averaged data on single levels from 1950 to 1978
source1 = ('adaptor.mars.internal-1639917199.7090092-16124-1-84aa04bd-3d6e-4c74-
a0fd-71450b44a889.nc');
%ERA5 monthly averaged data on single levels from 1979 to present
source2= ('adaptor.mars.internal-1639910457.3064284-4534-5-bda86fcf-da11-47b3-99d3-
9d2913d6fe49.nc');
t2m1=ncread(source1,'t2m');
t2m2=ncread(source2,'t2m');
long=ncread(source1,'longitude');
lat=ncread(source1,'latitude');
z=ncread(source1,'z');
deg011=ncread(source1,'deg01');
deg012=ncread(source2,'deg01');

dtim1= ncread(source1,'time');
dtim2= ncread(source2,'time');
dtim1=double(dtim1);
dtim2=double(dtim2);
t2m2=squeeze(t2m2(:,:,1,:));

deg012=squeeze(deg012(:,:,1,:));

deg01 = cat(3,deg011,deg012);
clear deg011 deg012

temp= cat(3,t2m1, t2m2);
clear t2m1 t2m2

t1=dtim1/24+datenum([1900 1 1 0 0 0]);
t2=dtim2/24+datenum([1900 1 1 0 0 0]);
tt = [t1 ;t2];
clear t1 t2
%
is50= find(tt >= datenum([1950 1 1 0 0 0])& tt < datenum([1960 1 1 0 0 0]));
deg0150=mean(deg01(:,:,is50),3);
is60= find(tt >= datenum([1960 1 1 0 0 0])& tt < datenum([1970 1 1 0 0 0]));
deg0160 =mean(deg01(:,:,is60),3);
is70= find(tt >= datenum([1970 1 1 0 0 0])& tt < datenum([1980 1 1 0 0 0]));
deg0170=mean(deg01(:,:,is70),3);
is80= find(tt >= datenum([1980 1 1 0 0 0])& tt < datenum([1990 1 1 0 0 0]));
deg0180=mean(deg01(:,:,is80),3);
is90= find(tt >= datenum([1990 1 1 0 0 0])& tt < datenum([2000 1 1 0 0 0]));
deg0190=mean(deg01(:,:,is90),3);
is2000= find(tt >= datenum([2000 1 1 0 0 0])& tt < datenum([2010 1 1 0 0 0]));
deg012000=mean(deg01(:,:,is2000),3);
is2010= find(tt >= datenum([2010 1 1 0 0 0])& tt < datenum([2020 1 1 0 0 0]));
deg012010=mean(deg01(:,:,is2010),3);
z=z(:,:,1);

g=9.80665;
hgpm=z./g;
Re=6378*10.^3;
hgeo= (hgpm.*Re) ./ (Re-hgpm); % geometric height from geopotential height h=
(Re*hg)/(Re+hg)
ho=hgeo + deg0150;
hrain=ho+360;
load coastlines
ho50=hgeo + deg0150;
hrain50=ho50+360;
ho70=hgeo + deg0170;
```



```

hrain70=ho70+360;

ho2010=hgeo + deg012010;
hrain2010=ho2010+360;

ho2000=hgeo + deg012000;
hrain2000=ho2000+360;
ho90=hgeo + deg0190;
hrain90=ho90+360;
ho80=hgeo + deg0180;
hrain80=ho80+360;

%anomalies ref 50 60 70
is50_70= find(tt >= datenum([1950 1 1 0 0 0])& tt < datenum([1980 1 1 0 0 0]));
deg0150_70=mean(deg01(:, :, is50_70), 3);

ho50_70=hgeo + deg0150_70;
hrain50_70=ho50_70+360;

%=====
% figure
figure
% subplot(2,2,1)
[~,cf]=contourf(long,lat, (hrain50-hrain50_70)');
xlabel('Longitude');
ylabel('Latitude');
title('hR anomalies 50s ')
caxis([-270 270])
colorbar
hold on
plot(coastlon, coastlat, '-w')
axis([min(long) max(long) min(lat) max(lat)])
hold off

%
is50= find(tt >= datenum([1950 1 1 0 0 0])& tt < datenum([1960 1 1 0 0 0]));
tm50=mean(temp(:, :, is50)-273.15, 3);
is60= find(tt >= datenum([1960 1 1 0 0 0])& tt < datenum([1970 1 1 0 0 0]));
tm60 =mean(temp(:, :, is60)-273.15, 3);
is70= find(tt >= datenum([1970 1 1 0 0 0])& tt < datenum([1980 1 1 0 0 0]));
tm70=mean(temp(:, :, is70)-273.15, 3);
is80= find(tt >= datenum([1980 1 1 0 0 0])& tt < datenum([1990 1 1 0 0 0]));
tm80=mean(temp(:, :, is80)-273.15, 3);
is90= find(tt >= datenum([1990 1 1 0 0 0])& tt < datenum([2000 1 1 0 0 0]));
tm90=mean(temp(:, :, is90)-273.15, 3);
is2000= find(tt >= datenum([2000 1 1 0 0 0])& tt < datenum([2010 1 1 0 0 0]));
tm2000=mean(temp(:, :, is2000)-273.15, 3);
is2010= find(tt >= datenum([2010 1 1 0 0 0])& tt < datenum([2020 1 1 0 0 0]));
tm2010=mean(temp(:, :, is2010)-273.15, 3);
is50_70= find(tt >= datenum([1950 1 1 0 0 0])& tt < datenum([1980 1 1 0 0 0]));
tm50_70=mean(temp(:, :, is50_70)-273.15, 3);
%
load coastlines

% figure 11
figure
% subplot(2,2,1)
[~,cf]=contourf(long,lat, (tm50-tm50_70)');
title('mean T(\circC) anomalies 50s')
caxis([-4 4])
colorbar
hold on
plot(coastlon, coastlat, '-w')
axis([min(long) max(long) min(lat) max(lat)])
xlabel('Longitude');
ylabel('Latitude');

```

```

caxis([-4 4])
colorbar
hold off
%%
code for Attenuation in Oslo Rain rate distribution from code done by collaboration
with my supervisor Terje Tjelta. Tipping bucket data rain rate calculation code and
the map showing the selected sites code is done by Terje Tjelta

metT = readtable('meteoStations4');%
sites = metT.Station;
Lats = metT.Latitude;
Lons = metT.Longitude;
Alts = metT.Height;
p = 0.01;
elev = 21;
hs = 0.2;
pol=0;
[ysrs,hR] = TestStationsrainHeightERA5();
% [ysrs2,R,stn] = TestStationsrainRateMonthlyData(p); %Monthly data
d2=load('TBstationsRRtrends.mat'); % Tipping bucket data

R=d2.varout(4).r01;
ysrs2=d2.varout(4).year;
isyear=ismember(ysrs,ysrs2);
hR=hR(:,isyear);
hR=hR/1000;

hs = 0.2;

[yt_1,Ap_1] =
satelliteAtten(0,Lats(1),Lons(1),hs,20,R,hR(1,:),ysrs2,pol,p,'Oslo');%sposition,lat,
lon,hsat,freq,rainrate,rainheight,year,polarization,p,station
[yt_2,Ap_2] =
satelliteAtten(0,Lats(1),Lons(1),hs,50,R,hR(1,:),ysrs2,pol,p,'Oslo');%sposition,lat,
lon,hsat,freq,rainrate,rainheight,year,polarization,p,station

figure
subplot(2,1,1)
i=find(yt_1>=1980 &yt_1<2020);

dataR = table(yt_1(i),Ap_1(i),'VariableNames',{'Year','Attenuation (dB)'});
modLin = fitlm(dataR);
plot(modLin,'linewidth',1)
grid on
title(' Satellite Link Attenuation (Tipping bucket) Oslo 20GHz' )

subplot(2,1,2)
i2=find(yt_2>=1980 &yt_2<2020);

dataR = table(yt_2(i2),Ap_2(i2),'VariableNames',{'Year','Attenuation (dB)'});
modLin = fitlm(dataR);
plot(modLin,'linewidth',1)
grid on

title(' Satellite Link Attenuation (Tipping bucket) Oslo 50GHz' )

```

```

%Satellite attenuation function
function [yt,Ap] =
satelliteAtten(sposition,lat,lon,hsat,freq,rainrate,rainheight,year,polarization,p,
station)
tau =polarization;
hS = hsat;
R=rainrate;
f = freq;

```

```

yt=year;
hR=rainheight;
satp=sposition;
phi=lat;

el=fn_elevangle(satp,lat,lon,hS); % Code by Terje T.
[a,b]= fn_itur_p838(f,el,tau); % code by Terje T.
% att= a*R.^b;

theta=el;
Ls=zeros(1,length(R));
for y=1:length(R)
    for m=1:length(theta)
        if theta(m)>5
            Ls(y) = (hR(y)-hS(m))./sind(theta(m));
        else
            Ls(y) = 2*(hR(y)-hS(m))./ ...
                sqrt(sind(theta(m)).^2+(2*(hR(y)-hS(m))./Re)+sind(theta(m))));
        end
    end
    LG= Ls.*cosd(theta);
    gamma=a.*R(y).^b;
    r1p = 1./(1+(0.78.*sqrt(LG.*gamma./f))-0.38.*(1-exp(-2.*LG)));

    zeta= atand((hR(y)-hS)./(LG.*r1p));
    LR= zeros(size(R));
    for m=1:length(theta)

        if zeta(y)>theta
            LR=(LG.*r1p)./cosd(theta(m));
        else
            LR=(hR(y)-hS(m))./sind(theta(m));
        end
        if abs(phi(m))<36
            x(m) = 36-abs(phi(m));
        else
            x(m)=0;
        end
    end

    end
end

V1p =1./(1+sqrt(sind(theta)).*((31.*(1-exp(-theta./(1+x)))) ...
    .*((sqrt(LR.*gamma))./f.^2)-0.45));
LE = LR.*V1p;
Alp= gamma.*LE;

Ap= nan(length(p),length(Alp));
for i=1:length(Alp)
    for j=1:length(p)
        if p(j)>=1 | abs(phi(j))>=36
            beta(i)=0;
        elseif (abs(phi(j))<36) & (p(j)<1) & (theta(j)>=25)
            beta(i) = -0.005.*(abs(phi(j))-36);
        else
            beta(i)= -0.005.*(abs(phi(j))-36) +1.8-4.25.*sind(theta(j));
        end
        Ap(j,i)= Alp(i).*(p(j)./0.01).^ ...
            (-0.665+0.033.*log(p(j))-0.045.*log(Alp(i))-beta(j).*(1-
p(j)).*sind(theta(j))));
    end
end
end
end

```

```

%% %% Terrestrial attenuation function
function [yt,Ap] =
terrestrialAtten(pathlg,freq,rainrate,year,polarization,p,station)
tau =polarization;
d = pathlg;
R=rainrate;
f = freq;
yt=year;
[a,b]= fn_itur_p838(f,0,tau);
att= a*R.^b;
if f>=10
    co= 0.12+0.4.*(log10(f/10).^0.8);
else
    co= 0.12;
end
c1=(0.07.^co).*(0.12.^(1-co));
c2=(0.855.*co)+(0.546.*(1-co));
c3=(0.139.*co)+(0.043.*(1-co));
r = 1./(0.477.*(d.^0.633).*(R.^(0.073.*b)).*(f.^0.123)-(10.579.*(1-(exp(-
0.024.*d)))));
deff = r.*d;
Alp= att.*deff;
Ap=Alp.*c1.*p.^(-(c2+(c3.*log10(p))));
figure

plot(yt,Ap,'-o','LineWidth',1.5)

grid on
ylabel('Attenuation (dB)')
xlabel(' Time')
lgd = legend(station);
title(lgd,'Location')
savefile=sprintf('TerrAttenuation%dghz%s%s',f,station,datestr(now));
save(savefile,'yt','Ap')

end

```

